THE BOEING COMPANY
AEROSPACE GROUP • P.O. BOX 3999 • SEATTLE, WASHINGTON 98124
AEROSPACE SYSTEMS DIVISION

M.I.

January 16, 1969
IN REPLY REFER TO
2-1120-1-247-OR

National Aeronautics and Space Administration
George C. Marshall Space Flight Center
Marshall Space Flight Center, Alabama 35812

Attention: PR-RC

Subject: Contract NAS 8-20901 - "Design and Development of Techniques for Fabrication of Cryogenic Tank Support Structures for Long Term Storage in Space Flights" - Phase I Report

Gentlemen:

The Boeing Company, Aerospace Systems Division, transmits herewith ten (10) copies of its Phase I Report in accordance with the requirements of subject contract.

Any questions or comments concerning this matter should be directed to the attention of A. R. Selin at The Boeing Company, Aerospace Group, Kent Facility, P. O. Box 3999, Seattle, Washington 98124, telephone 773-4300 (area code 206).

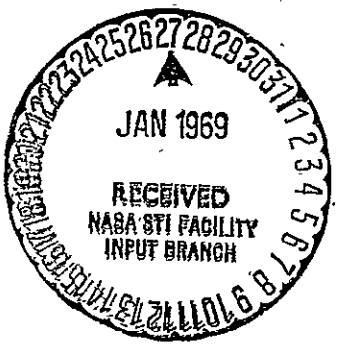

Sincerely,

THE BOEING COMPANY
Aerospace Group

pa L. E. O'Toole
Contracts Manager - Aerospace Systems
Product Development and Technology

Enclosures: Phase I Report (10 copies)

cc: R-P&VE-SAE (Mr. J. M. Walters)

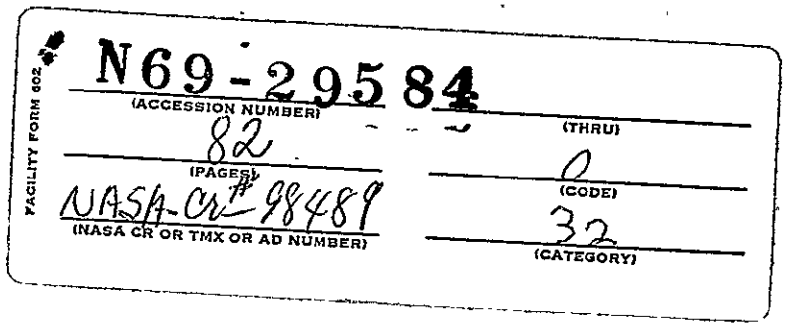

C01

DESIGN AND DEVELOPMENT OF TECHNIQUES FOR FABRICATION OF CRYOGENIC TANK SUPPORT STRUCTURES FOR LONG TERM STORAGE IN SPACE FLIGHTS

Phase I Report
April 1 through November 1, 1968

Prepared by

THE BOEING COMPANY
Space Division
Seattle, Washington

C. F. Tiffany - Program Manager
D. H. Bartlett - Technical Leader

Prepared for
NATIONAL AERONAUTICS AND SPACE ADMINISTRATION
George C. Marshall Space Flight Center
Huntsville, Alabama

TABLE OF CONTENTS

1.0 INTRODUCTION

This report describes the results of a study to determine the least weight method of constructing a conical support for the 32 ft diameter modular Nuclear Vehicle LH_2 tank. Both metallic and nonmetallic materials were considered as well as various methods of construction, i.e., honeycomb sandwich, stiffened skin, and corrugations. The work described herein comprises Phase I of Contract NAS 8-20901. The period of performance was April through October of 1968.

Initial effort consisted of optimizing various construction methods to yield a structure of minimum cross sectional area. Detail designs of the optimized structural concepts were then developed and a weights analysis was made. Thermal conductance was calculated and in turn, was used to determine LH_2 boil off losses for a specific mission duration. The summation of LH_2 boil off weight and structural support weight provided a means of comparing concept efficiency.

Fiberglass honeycomb sandwich construction was shown to be the most efficient for the tank support. A subscale support utilizing the same construction was designed for the MSFC 105 inch diameter LH_2 test tank. Phase II of this program consists of fabrication and delivery of the subscale conical support.

2.0 STUDY PROGRAM

2.1 Ground Rules

The design envelope, loads, and load factors to be used in the study were selected by MSFC. The envelope is depicted in Figure 1.

Methods of construction to be considered were honeycomb sandwich, Zee stiffened skin, bar stiffened skin, hat stiffened skin, and corrugations. Both metallic and nonmetallic materials would be assumed for each construction concept.

Vertical splice joint and top and bottom edge attachment details would be developed for each structural concept. The optimum number of cone segments was to be determined based on parameters such as heat leak, weight, fabrication ease, and simplicity of assembly.

Thermally induced stresses would be considered in the designs. There was no design stiffness requirement.

MSFC was interested principally in obtaining a test part (Phase II) that would typify the heat leak and insulation assembly problems of the 32 ft diameter conical support. Therefore, the subscale support would be identical in length and cross sectional geometry to provide a heat leak per inch of circumference typical of the full size cone.

2.2 Materials

Titanium alloys 6Al-4V and 5Al-2.5Sn were the candidate metallic materials considered in the study. 6Al-4V was used in the annealed condition to simplify fabrication and because the higher strength of heat treated material was not needed.

Fiberglass reinforced epoxy plastic was the nonmetallic material selected. This material had been shown to be suitable for cryogenic applications in

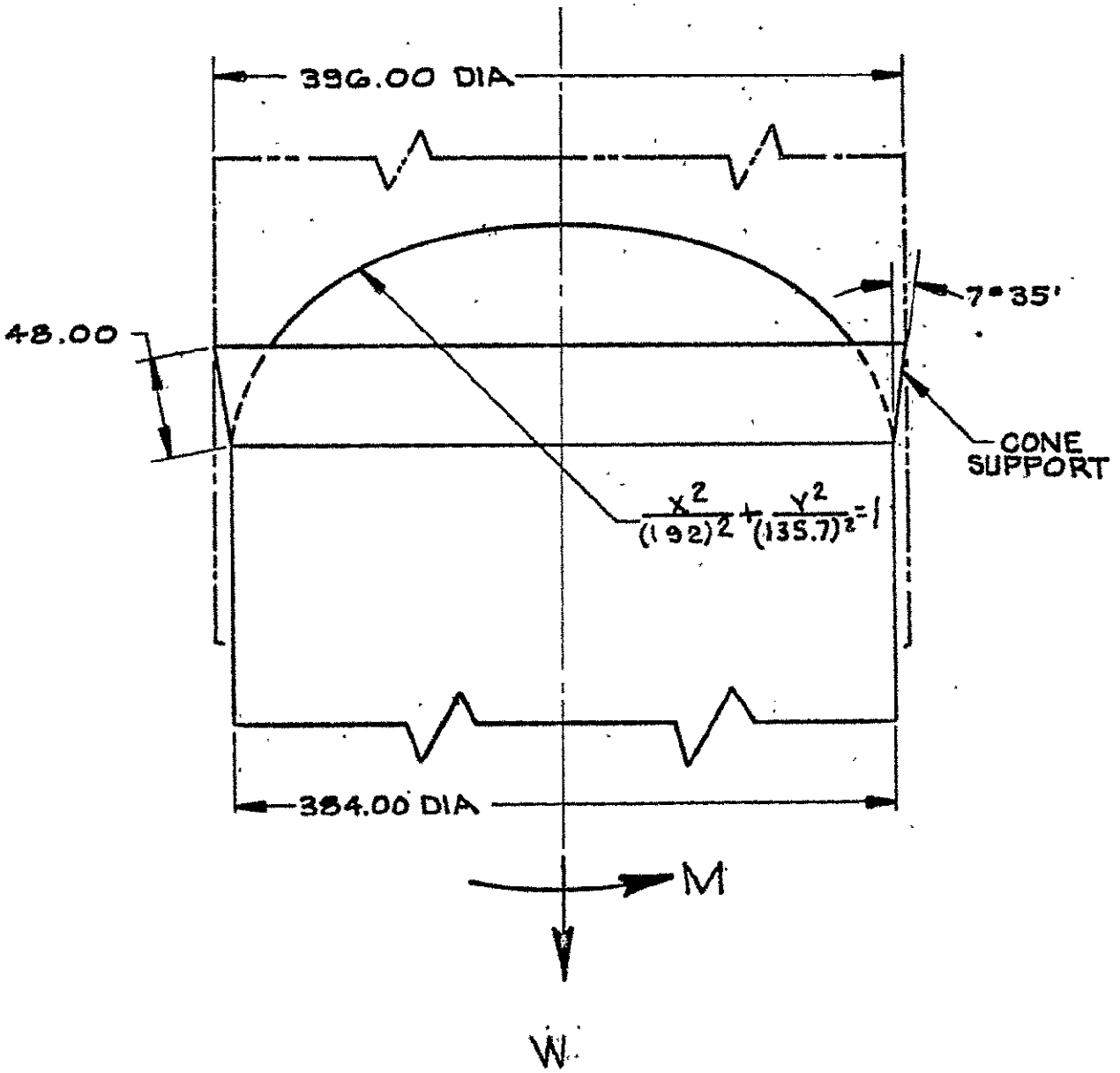
396.00 DIA
48.00
7°35'
CONE SUPPORT
$\frac{x^2}{(192)^2}+\frac{y^2}{(135.7)^2}=1$
384.00 DIA
M
W

FIGURE 1

previous studies (References 1 and 2). The material form was style 181-"S" glass cloth. Honeycomb sandwich designs utilized fiberglass core impregnated with phenolic resin (HRP).

The allowable design properties of the materials used in the program were as follows:

Style 181-S/901 Fiberglass Cloth Preimpregnated with U.S. Polymeric E-787 Epoxy Resin or Equivalent (Ref. 1)

ITEM	PARALLEL lbs/in^2	45° lbs/in^2	NORMAL lbs/in^2
F_{tu}	65,000*	14,196	65,000
F_{cu}	58,225	26,782	53,118
F_{bry}	31,810	--	--
E	3,062,848	1,552,301	2,837,151
G	1,500,000	400,000	1,500,00
F_{su}	11,000	27,000	11,000
Interlaminar Shear	6,455	--	--
Thermal Conductivity $\frac{BTU\text{-}in}{In^2\text{-}Hr\text{-}°F}$	0.013	--	--

μ = 0.125 Density = 0.066 lbs/in^3 * Adjusted by Boeing

6Al-4V Titanium - Annealed

F_{tu} = 134,000 lbs/in^2 F_{bru} = 252,000 (e/D = 2.0) lbs/in^2

F_{cy} = 132,000 lbs/in^2 F_{bry} = 208,000 (e/D = 2.0) lbs/in^2

F_{su} = 79,000 lbs/in^2 μ = .30

E = 16.4 x 10^6 lbs/in^2 Density = .16 lbs/in^3

G = 6.2 x 10^6 lbs/in^2 Thermal Conductivity = 0.24 $\frac{BTU\text{-}in}{in^2\text{-}Hr\text{-}°F}$

2.3 Loads

Three loading conditions were considered. These were:

Load Condition 1 (maximum q) limit

W = 300,000 lbs

M = 106.1×10^6 in-lbs

Axial Acceleration = 2.0 G
Lateral Acceleration = 0.5 G
} Combined

Load Condition 2 (S-IC Burnout) limit est.

W = 300,000 lbs

Axial Acceleration = 5.0 G

Load Condition 3 (S-IC Cutoff) limit

W = 300,000 lbs.

Axial Acceleration = -2.5 G

Factors of Safety were:

Ultimate = 1.4

Yield = 1.1

Shell loads were determined from the following expressions:

$$N_x = \frac{P}{\pi D \cos \theta} \pm \frac{4M}{\pi D^2 \cos \theta}$$ - Tension or Compression Loading lbs/in

$$N_{xy} = \frac{V}{\pi R}$$ Shear Flow - lbs/in.

where P = total axial load

V = shear load due to lateral acceleration.

The shell loads for the three design conditions are tabulated below:

CONDITION	IN SHELL PLANE LOADING LBS/IN.	LIMIT		ULTIMATE	
		396"D TOP	384"D BOTTOM	396"D TOP	384"D BOTTOM
1 (Max. q)	Compression	-382	-364	-535	-509
	Tension	1355	1367	1897	1914*
	Shear	241	249	338	348*
2 (Burnout)	Compression	--	--	--	--
	Tension	1216	1254	1703	1756
	Shear	--	--	--	--
3 (Cutoff)	Compression	-608	-627	-851	-878*
	Tension	--	--	--	--
	Shear	--	--	--	--

* Critical Ultimate Design Conditions

2.4 Structural Concept Optimization

2.4.1 Corrugated Structure

The 60° corrugation studied in the program consisted of a constant thickness sheet formed into a repeating series of equilateral corrugations. There were no face sheets on the corrugation surfaces and circumferential rings were used at each end of the conical frustum. This type of design appeared well suited to cryogenic applications where large thermal gradients between support structure and the tank could produce significant thermal stresses. The corrugated structure would permit an "accordion action" of the panel and thus relieve stresses due to thermal gradients.

In the tank support areas pressure loads did not exist and the primary loading was axial plus lateral shear. A corrugated sheet without face panels is essentially unidirectional. The closely spaced "stiffeners" provided high compressive strength and all the material was acting in both compression and shear.

The corrugation could resist crack growth and provide a fail safe design. The longitudinal stiffness of the panel was ideal from a boundary layer noise viewpoint. The attachment of the corrugation along the edges presented an important and difficult area for detail design. The panel was flexible in the curved direction so that for single curvature the manufacturing characteristics resembled that of stringer stiffened construction.

ANALYSIS CRITERIA

The following assumptions were made in the analysis:

1. Whenever "Optimization" was mentioned directly or in any of its forms, it meant that a minimum cross sectional area (weight, heat flow) was effected for a given material.
2. The conical frustum was designed as an equivalent cylinder and R was the radius of curvature of the small end normal to the surface and L was the slant height of the conical frustum. Test data (Ref. 3) indicated that buckling occurred when the maximum meridional stress (at the small end of the cone) reached the critical value for a cylinder having curvature of the cone and a thickness equal to that of the cone.
3. The maximum compression loading that would occur in the shell due to combined bending plus axial load was treated as acting uniformly around the circumference of the shell for general instability analysis. (This was conservative as shown in Ref. 4).)
4. The critical shear instability load was equivalent to a long corrugated flat panel with simply supported edges subjected to the maximum shear stress existing in the conical frustum.
5. The interaction of shear and compression was negligible. (The maximum shear stress occurred at 90° from the maximum axial stress and was zero at point of maximum compression load.)
6. The equilateral corrugation shape was optimum (all elements had the same

critical stress) and the angle of corrugation $\theta = 60°$ was near optimum (Ref. 5).

7. General or panel instability would occur as column instability.
8. Stresses would remain elastic.
9. Distortion effects due to curvature were negligible.
10. The optimum cross sectional geometry had been achieved when the column stress and the crippling stress were equal.
11. The structure existing on the tank at the support interface would act as a ring to support the corrugation along with the corrugation edge member.
12. The overall height from the tank-cone intersections at the 396 inch and 384 inch diameters were conservatively used as the effective height of the conical frustum.

EQUILATERAL CORRUGATION SECTION PROPERTIES

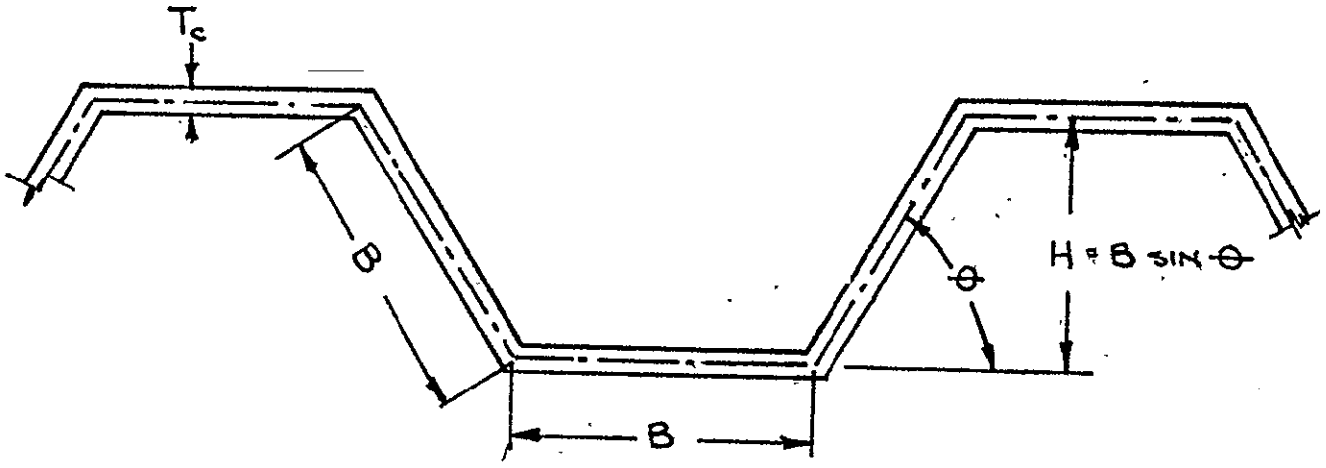

General Section Properties

$$I = \frac{T_c B^2}{3} \left(\frac{\sin^2 \theta}{1 + \cos \theta}\right) = \text{Moment of inertia per inch}$$

$$A = 2 \left(\frac{T_c}{1 + \cos \theta}\right) = \text{Cross sectional area per inch}$$

$$\rho = \sqrt{I/A} = \frac{B \sin \theta}{\sqrt{6}} = .408\ B \sin \theta = \text{Radius of Gyration per inch}$$

60° Corrugation Properties

$$\rho = \frac{1}{2\sqrt{2}} B = .354\ B$$

$$A = 4/3\ T_c = 1.333\ T_c$$

$$I = 1/6\ T_c\ B^2 = .1666\ T_c\ B^2$$

FAILURE MODES

Local Instability - Crippling

In order to predict the local crippling of the corrugation skin, it was assumed that the edges were simply supported and the flats of the corrugations were long plates. The critical local crippling stresses were:

Compression: $F_{ccr} = \frac{4.0\ \pi^2\ E}{12\ (1 - \mu^2)} \left(\frac{T_c}{B}\right)$ Ref. 6

Shear: $F_{sccr} = \frac{5.35\ \pi^2\ E}{12\ (1 - \mu^2)} \left(\frac{T_c}{B}\right)^2$ Ref. 6

General Instability - Panel Buckling

General instability or panel buckling consists of Euler column buckling between the end ring supports for compression load. The panel can also fail in shear general buckling. Assuming simply supported end conditions the following was used to predict the buckling stress:

Compression: $F_{col} = \frac{\pi^2\ E}{(L/\rho)^2}$ Ref. 7

Reference 8 was used for the analysis of corrugated shear webs. This analysis

was verified with experimental data. In the design of corrugated shear webs, it was necessary to consider the flexural stiffness of the web in the vertical and horizontal directions. The formula for critical shear load per inch is:

$$N_{xy} = \frac{4 K_s \sqrt{D_1 D_2^3}}{L^2}$$ Ref. 8

where:

D_1 = plate flexural stiffness in circumferential direction = $E T_c^3 \times (1 + \cos \theta)/24$

D_2 = plate flexural stiffness in depthwise direction = $E A \rho^2$ = $\frac{E B^2 \sin^2 \theta T_c}{3 (1 + \cos \theta)}$

T_c = corrugation skin thickness - in.

B = corrugation width of flat - in.

L = corrugation length between fasteners - in.

K_s is the shear buckling coefficient which was dependent upon the radius of gyration - ρ and the edge restraint ε. Assuming simply supported edges, K_s was found from Figure 2. The parameter, $\lambda/L \sqrt[4]{D_2/D_1}$, was taken as near unity since the stiffness D_2 was several orders of magnitude greater than D_1; hence the quantity λ (wave length)/L was small. This gave K_s = 8.15 for a simply supported edge condition. Substitution of the corrugation parameters gave:

$$N_{xy} = \frac{.7928 K_s E T_c^{1.5} B^{1.5} \sin \theta^{1.5}}{L^2 (1 + \cos \theta)^{.5}}$$

$$F_{scr} = \frac{.7928 K_s E T_c^{.5} B^{1.5} \sin \theta^{1.5}}{L^2 (1 + \cos \theta)^{.5}}$$

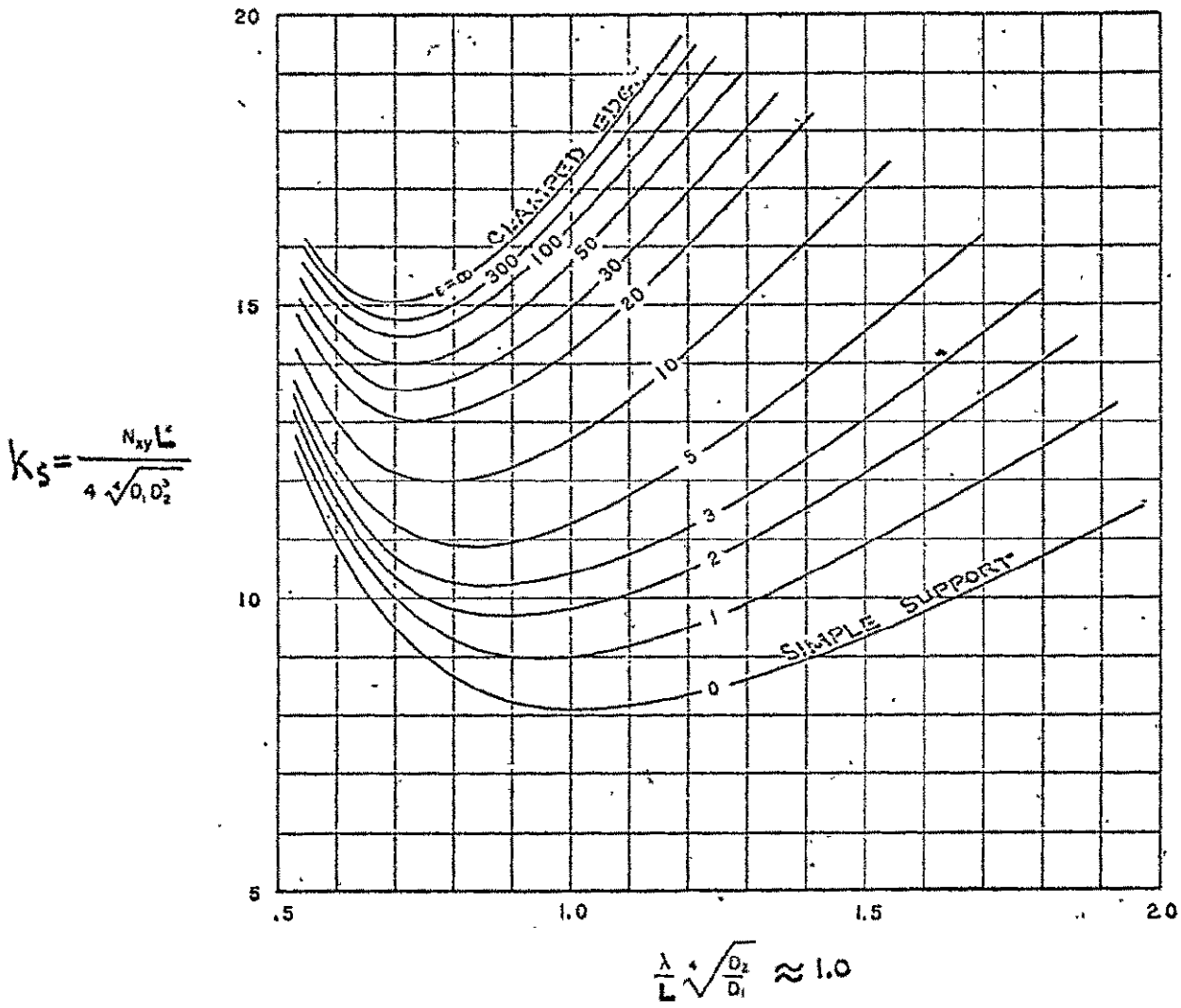

Figure 2.- Shear buckling coefficients of long corrugated plates with nondeflecting edge supports.

FIGURE 2

For 60° Corrugation

$$F_{scr} = \frac{.5217\ K_s\ E\ T_c^{.5}\ B^{1.5}}{L^2}$$

For Simply Supported Edges $K_s = 8.15$

$$F_{scr} = \frac{4.25\ E\ T_c^{.5}\ B^{1.5}}{L^2}$$

OPTIMIZATION PROCEDURE

In order to arrive at an optimum corrugation configuration, the critical stress levels for Euler and local crippling were equated to one another. The constraints that the corrugation must not fail by local shear crippling or general shear buckling were imposed; however, these did not become active in this design. This is because the shear loading was of a low enough magnitude. The shear and compression loading was not coupled since the maximum valued occurred at different locations.

Equating $F_{ccr} = F_{col}$

$$\frac{4.0\ \pi^2\ E\ T_c^2}{12\ (1-\mu^2)\ B^2} = \frac{\pi^2\ E\ \rho^2}{L^2}$$

Since $\rho = \frac{1}{2\sqrt{2}} B$ for the 60° corrugation being considered here, the above equation was reduced to

$$B^2 = T_c\ L \sqrt{\frac{32}{12\ (1-\mu^2)}}$$

Equating actual stress level with the local crippling stress:

$$f_c = \frac{N_x}{4/3\ T_c} = \frac{3\ N_x}{4\ T_c} = \text{actual stress level lbs/in}^2$$

$$\frac{3\ N_x}{4\ T_c} = \frac{4.0\ \pi^2\ E\ T_c^2}{12\ (1 - \mu^2)\ B^2}$$

$$B^2 = \frac{16\ \pi^2\ E\ T_c^3}{36\ N_x\ (1 - \mu^2)}$$

Equating the B^2 terms:

$$T_c L \sqrt{\frac{32}{12\ (1 - \mu^2)}} = \frac{16\ \pi^2\ E\ T_c^2}{36\ N_x\ (1 - \mu^2)}$$

$$T_c^2 = \frac{36\ L\ N_x\ (1 - \mu^2)\ 32}{16\ \pi^2\ E \sqrt{12\ (1 - \mu^2)}}$$

$$T_c = .6102\ (1 - \mu^2)^{1/4} \sqrt{\frac{N_x L}{E}}$$

Therefore, with the ring spacing given, the optimum corrugation skin thickness was calculated from the above equation. Knowing T_c, the other corrugation geometry was calculated by:

$$B = \frac{1.278 \sqrt{T_c L}}{(1 - \mu^2)^{1/4}}$$

CORRUGATION RING REQUIREMENTS

An investigation of ring requirements was made, employing analytical methods for optimizing ring quantities. The study results are discussed in the following paragraphs.

Experimental evidence had indicated that a certain ring stiffness was required

to force an inflection point of the buckling pattern at the ring support. This required ring stiffness was:

$$E_r I_r = 3 \times 10^{-5} \frac{\pi N_x D^4}{L} \quad \text{(Reference 9)}$$

This was two times the requirement recommended by Shanley (Reference 10) for the monocoque shells that have hoop stiffness.

To optimize the 60° corrugation, using the Reference 9 approach, the following procedure was used:

a. Design the corrugation without any intermediate rings to reduce the unsupported length and calculate the resulting weight.

b. Add one ring and design the corrugation based on the reduced value of unsupported length and calculate the resulting weight of the corrugation plus the ring.

c. Continue adding the rings until an increase in total weight is noted. At this point, the optimum ring spacing has been found.

This analysis showed that it was not efficient to add rings to the tank support. The ring requirements appeared to be too extreme for this particular application of large diameters. The ring requirements were investigated by another method (Reference 11). This method treated the corrugation as a beam on an elastic foundation. The ring spring stiffness required to force an inflection point of the buckling pattern at the point of support was taken as $K = 23\ E\ I_R/R^3$ where I_R was the moment of inertia of the ring frame and

$$P_{cr} = 2\sqrt{\frac{EIK}{a}}$$

where EI was the corrugation flexural stiffness and "a" was the ring spacing.

This method yielded realistic ring requirements but, as before, it was more weight efficient to delete the reinforcing rings.

RESULTS

The final optimized sizing of corrugated titanium and fiberglass structure is shown in Figures 3 and 4 for:

N_x = -851 lbs/in applied ultimate compression loading
+1897 lbs/in applied ultimate tension loading

N_{xy} = 338 lbs/in applied ultimate shear loading

R_{eff} = 193.69 in. normal to surface at small end

L = 45.47 in. slant height

The fiberglass support had more than twice the cross sectional area; however, the weight was less.

2.4.2 Stiffened Construction

ANALYSIS

It has been established that the most efficient structure is that in which every type of instability which could cause failure occurs simultaneously.

The stringer-skin combination can develop several separate types of instability, which may be coupled to a greater or lesser degree (Reference 12).

(a) Skin buckling (or initial buckling). This generally involves waving of the skin between stringers in a half-wavelength comparable with the stringer pitch. There will also be a certain amount of waving of the stringer web and lateral displacement of the free flange. For some proportions the latter may become larger than the skin displacements, and the mode becomes more torsional or local in nature (see (b) and (c)).

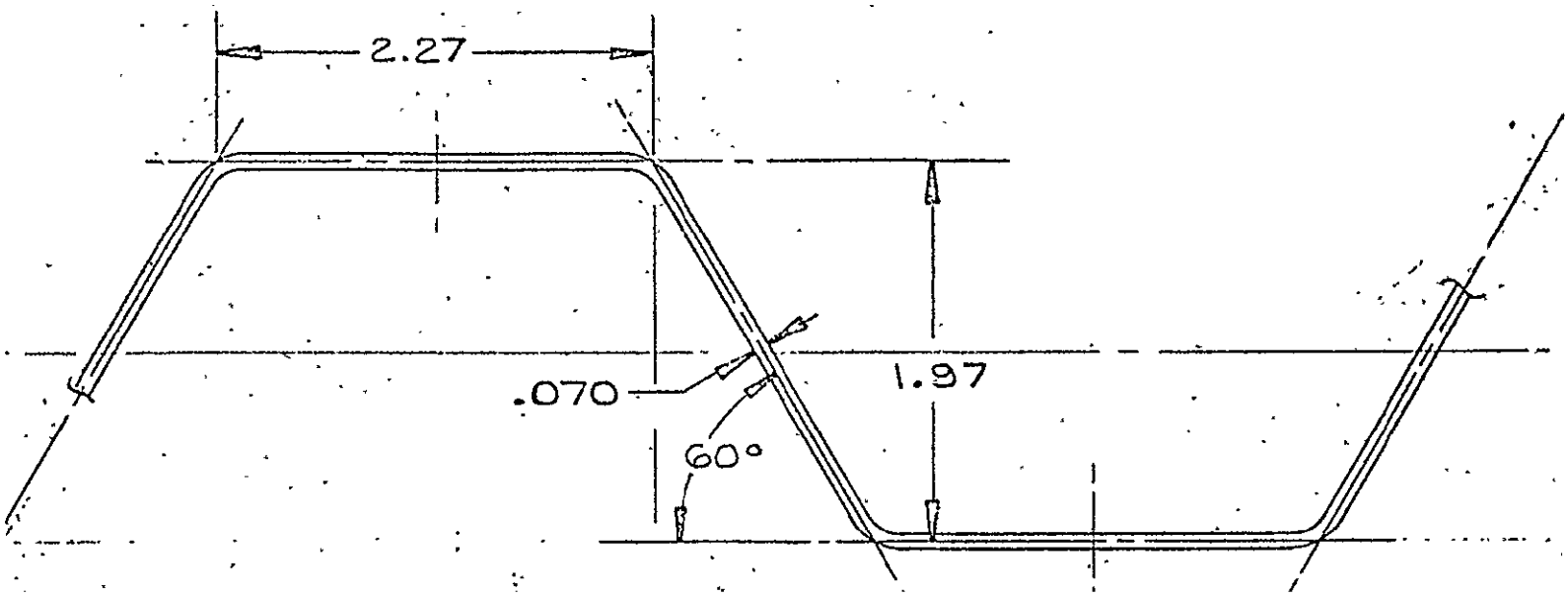

APPLIED ULT LOAD ~ COMPRESSION = 851.45 LBS/IN
SHEAR = 338.0 LBS/IN

EFF AREA=.0921 IN^2/IN WEIGHT = .0061 LBS/IN CIRCUM* LENGTH

APPLIED ULT. COMPRESSION STRESS	=	9,249 LBS/IN^2
ALLOWABLE COMPRESSION CRIPPLING STRESS	=	9,249 LBS/IN^2
ALLOWABLE COMPRESSION BUCKLING STRESS	=	9,249 LBS/IN^2
APPLIED ULT. SHEAR STRESS	=	4,890 LBS/IN^2
ALLOWABLE SHEAR CRIPPLING STRESS	=	12,371 LBS/IN^2
ALLOWABLE SHEAR BUCKLING STRESS	=	5,553 LBS/IN^2
APPLIED ULT: TENSION STRESS	=	27,500 LBS/IN^2
ALLOWABLE ULT. TENSION STRESS	=	65,000/ $LBS\cdot IN^2$

FIBERGLASS CORRUGATION

FIGURE 3

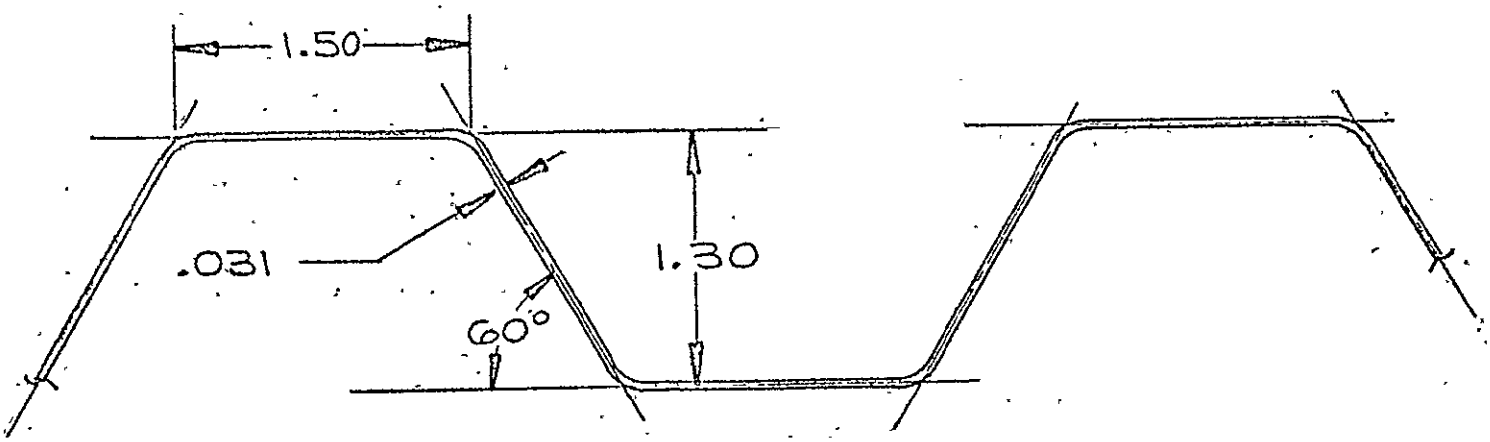

APPLIED ULT LOAD ~ COMPRESSION = 851.45 LBS/IN
SHEAR = 338.0 " "

EFF AREA = .0413 IN²/IN WEIGHT = .0066 LBS/IN CIRCUM & LENGTH

APPLIED ULT. COMP. STRESS	= 20,063 LBS/IN²
ALLOWABLE COMPRESSION CRIPPLING STRESS	= 25,207 LBS/IN²
ALLOWABLE COMPRESSION BUCKLING STRESS	= 22,055 LBS/IN²
APPLIED ULT SHEAR STRESS	= 10,906 LBS/IN²
ALLOWABLE SHEAR CRIPPLING STRESS	= 33,715 LBS/IN²
ALLOWABLE SHEAR BUCKLING STRESS	= 10,910 LBS/IN²
APPLIED ULT. TENSION STRESS	= 61,000 LBS/IN²
ALLOWABLE ULT TENSILE STRESS	= 134,000 LBS/IN²

TITANIUM CORRUGATION

FIGURE 4

(b) Local instability. Secondary short-wavelength buckling may take place in which the stringer web and flange are displaced out of their own planes in a half-wavelength comparable with the stringer depth. There will be smaller associated movements of the skin and lateral displacements of the stringer free flange.

(c) Torsional instability. The stringer rotates as a solid body about a longitudinal axis in the plane of the skin, with associated smaller displacements of the skin normal to its plane and distortions of the stringer cross-section. The half-wavelength is usually of the order of three times the stringer pitch.

(d) Flexural instability. Simple strut instability of the skin-stringer combination in a direction normal to the plane of the skin. There may be small associated twisting of the stringers. The half-wavelength is generally equal to the frame spacing.

(e) Inter-rivet buckling. Buckling of the skin as a short strut between rivets: this can be avoided by using a sufficiently close rivet pitch along the stringer.

(f) Wrinkling. A mode of instability similar to inter-rivet buckling, but analogous to wrinkling of a sandwich structure, in which the skin develops short-wavelength buckling as an elastically supported strut. For all practical skin-stringer combinations it can be avoided by keeping the line of attachment very close to the stringer web.

Failure of Stringers

When the skin stringer combination approaches its Euler instability stress, development of instabilities (a), (b), (c), (e), or (f) will so reduce the flexural stiffness as to cause premature collapse.

Buckled Skin Versus Unbuckled Skin Designs

If the Euler instability stress is reasonably remote, instability (a) (skin buckling) will not precipitate failure, and the structure will carry increased load, with the skin buckled until failure occurs by the onset of instability (b), (c), (e), or (f). In general an excessive margin of flexural stiffness is needed to prevent failure due to any of these latter four modes.

By letting failure occur at more than about three times the skin buckling stress, stringers are relatively sturdy and coupling between skin buckling and stringer local distortion is negligible. It has also been established that coupling of modes reduces the lower instability stress and raises the higher, and thus leads to a less efficient design. Efficient designs can be obtained, however, by either not allowing the skin to buckle at all, or letting the skin buckle at a comparatively low stress.

The unbuckled skin design was used throughout this study. While this type of structure was not quite as efficient as the buckled skin design for load magnitudes that were low, this structure did offer increased shear stiffness over the buckled design. The structure was analyzed thoroughly to prevent any instabilities from occurring which would cause premature failure.

OPTIMIZATION PROCEDURES

The optimization used to determine the minimum cross sectional area made use of:

1. Multiple load conditions of compression plus shear
2. Local and general instability analysis
3. Imposed constraints such as:
   a. Minimum gage requirements
   b. Minimum stiffener moment of inertia required to break up panels for shear instability

c. Minimum stiffener gage requirements to restrain shear buckles

d. Torsional instability requirements for zee sections

e. Minimum size of outstanding legs of zee sections to offer support to vertical legs.

All elements of the stiffened construction were checked for local crippling by the following formulas:

$$\text{(Compression)} \quad F_{ccr} = \frac{K E}{12 (1 - \mu^2)} (t/b)^2$$

and

$$\text{(Shear)} \quad F_{scr} = \frac{K_s E}{12 (1 - \mu^2)} (t/D)^2$$

where

$K_s = 5.35 + 4(D/L)^2$

D = stiffener spacing

L = length of panel

b = width of element

t = thickness of element

The panel general instability was checked using the Euler column formula with simply supported ends.

$$F_{col} = \frac{\pi^2 E}{(L/\rho)^2}$$

The optimization was performed with a digital computer using an iterative procedure. Iterations were performed on the geometrical variables over the range of interest. The configuration which provided the minimum area while satisfying all constraints was saved as the final optimum configuration.

The restraints imposed and associated formulas follow:

Outer Flange Minimum Length Restraint

The outer lip of the zee stiffner should not be shorter than necessary to offer stability to the flange as shown below:

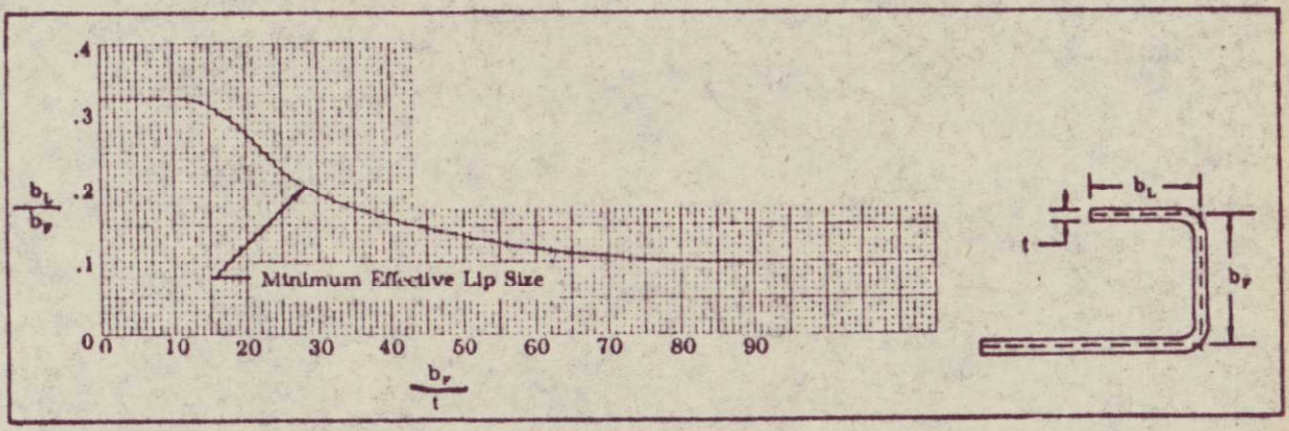

Above Minimum Effective Curve: Consider lip as a flat segment with 1 edge free. Consider adjacent flange as having 0 edges free.

Below Minimum Effective Lip Curve: Consider the flange adjacent to lip as segment with 1 edge free. The length of the flange becomes $b = b_F + b_L$. Use this b in analyzing the flange.

Shear Restraints

(A) Local Shear Instability

The sheet material was not allowed to buckle between stiffening members. The allowable shear local instability stress was obtained by

$$F_{sccr} = \frac{5.35\,\pi^2\,E}{12\,(1-\mu^2)}\,(t/D)^2$$

(B) Stiffener Moment of Inertia Requirement with Non-buckling Web

The minimum required value of stiffener moment of inertia to prevent failure due to shear loads was computed using the following formula:

$$I_{s\ req'd} = D/t \left[\frac{L^2\ t\ fs}{16E}\right]^{4/3}$$

where fs was the shear stress in the web.

(C) Stiffener Flange Thickness Required Next to Web

The web stiffeners were required to decrease the size of the web panels to prevent (1) buckles from forming across the stiffener, and (2) the web from buckling as a whole section. The allowable shear instability stress was determined from

$$F_{scr} = \frac{\pi^2\ k_s\ E}{12\ (1-\mu^2)}\ (t/D)^2$$

where $k_s = 1.1064\ K_s$

K_s was the plate shear buckling coefficient derived from the following graph:

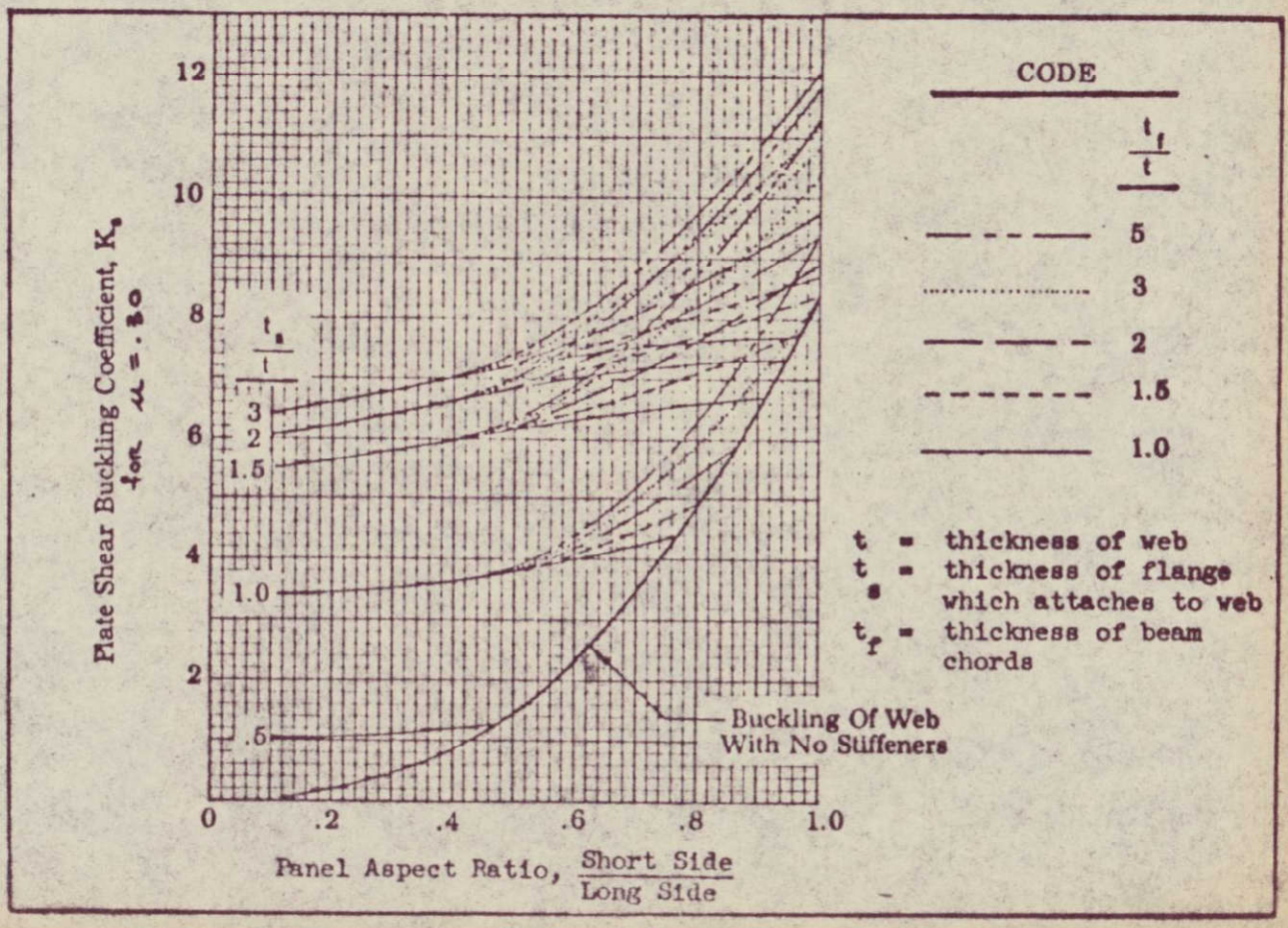

Torsional Instability Restraint

The torsional instability restraint was applied to the stiffened construction. The hat section and bar section stiffened structure did not require this restraint.

Torsional failure of stiffened panels was investigated by making the assumption that the stiffener with some adjacent skin acted as a column. This was done to simplify a difficult problem. A rigorous solution (Reference 13) to the problem of a stiffened panel failing torsionally was obtained by assuming the stiffener to be forced to rotate about a point in the plane of the skin along the line of attachment. The solution obtained by the rigorous treatment yielded a higher allowable critical load.

The J-section shown below was used to approximate sections from stiffened panels of zee sections attached to skin. The length "c" was replaced by an effective width of plate. The attached flange of the zee section was distributed along the effective length so that the thickness t_2 became:

$$t_2 = t_{skin} + \frac{A_{flange}}{\text{eff. width}}$$

The constants x_o, y_o, and Γ for the sheet and stiffener were computed from the equations given below. The critical stress was then computed by calculating the equivalent slenderness ratio and substituting into the Euler column formula. The equations for x_o and y_o yielded exact solutions, whereas, the equation for Γ was an approximation.

J - Section

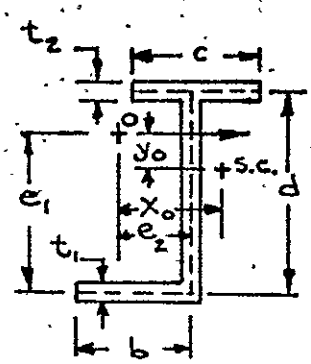

$$x_o = e_2 + \frac{b^2 dt_1}{I_x I_y - I_{xy}^2}\left[\frac{I_y e_1}{2} - I_{xy}\left(\frac{e_2}{2} - \frac{b}{3}\right)\right]$$

$$y_o = e_1 - d + \frac{b^2 dt_1}{I_x I_y - I_{xy}^2}\left[\frac{I_{xy} e_1}{2} - I_x\left(\frac{e_2}{2} - \frac{b}{3}\right)\right]$$

where:

$$I_1 = \frac{t_1 b^3}{12} \quad , \quad I_2 = \frac{t_2 c^3}{12}$$

$$\text{⊤} = \frac{d^2 I_1 I_2}{I_1 + I_2} \qquad \text{(Approximate solution)}$$

It was assumed that centrally loaded columns would buckle in the plane of a principal axis without rotation of the cross section, but experience revealed that columns having open cross sections showed a tendency to bend and twist simultaneously under axial load. The actual critical load of such columns, due to their small torsional rigidity, could be less than the critical load predicted by the generalized Euler formula.

To check the torsion failure mode it was necessary to compute a radius of gyration which yielded the greatest slenderness ratio which could then be used to predict a strength. The radii of gyration which were checked were the usual ρ_{xx} and ρ_{yy} and an equivalent radius of gyration. To compute the

equivalent radius of gyration the following was needed:

$$\rho_\theta = \sqrt{\frac{c_w \Gamma}{I_o} + \frac{c_\theta L^2 GJ}{\pi^2 E_c I_o}} \quad \text{in.}$$

where J and I_o were cross sectional properties defined below:

J was the torsion constant of St. Venant (For open thin walled sections $J = \frac{1}{3}\sum mt^3$ where m was the middle line length of each flange or web and t the thickness).

$$I_o = I_{xx} + I_{yy} + A\,(y_o^2 + x_o^2) \quad \text{in.}^4$$

where y_o, x_o were components of distance from the shear center to the centroid.

The c's were fixity coefficients defined as follows:

c_w = Coefficient indicating amount of fixity against warping.

c_θ = Coefficient indicating amount of fixity against twisting.

The coefficients c_w and c_θ are usually assumed as equal to one.

If $\mu = 0.3$ and $\frac{G}{E_c} = \frac{1}{2(1+\mu)}$ then

$$\rho_\theta = \sqrt{\frac{c_w \Gamma}{I_o} + .039\,\frac{c_\theta L^2 J}{I_o}}$$

If the cross section of the column had no axis of symmetry, the modes of failure were dependent on one another. The slenderness ratio was obtained as follows:

$$\frac{L}{\rho_e}$$

where $(\rho_e)^2$ was the smallest root of a cubic equation given in Reference 14.

RESULTS

Figures 5, 6, 7, 8, 9, and 10 show the optimized configurations of hat, bar, and zee stiffened panels of both titanium and fiberglass construction. In all cases the cross sectional area of fiberglass was greater than in the titanium counterparts; however, the fiberglass parts weighed less.

2.4.3 Honeycomb Construction

ANALYSIS

A study of the effects of orientation of the honeycomb core ribbon was made on allowable buckling strength and heat flow. The shear modulus of the core was approximately twice as great in the direction of the ribbon as in a direction perpendicular to the ribbon. If the ribbon were oriented in the circumferential direction of the cone, the heat flow was substantially reduced whereas, the allowable longitudinal buckling load was only slightly reduced.

If the heat flow of the core was calculated for the cross sectional area of the foil material and developed length, it was found that the core had a heat flow 1.5 times greater when the ribbon was oriented in the longitudinal direction than in the circumferential direction. If the core ribbon developed length was not used in the heat flow calculations, the heat flow difference between core direction became 1.732 instead of 1.5. Therefore, the designs were made with the ribbon oriented in the circumferential direction. Figure 11 shows core dimensional relationships. The equations used for calculating core heat flow were:

Using direct length

$$\text{Effective cross sectional core area perpendicular to ribbon direction} = \frac{\rho_c \times T_c}{3991 \times \rho_f}$$

$$\text{Core heat flow} = \frac{K_c \times \rho_c \times T_c}{3991 \times \rho_f}$$

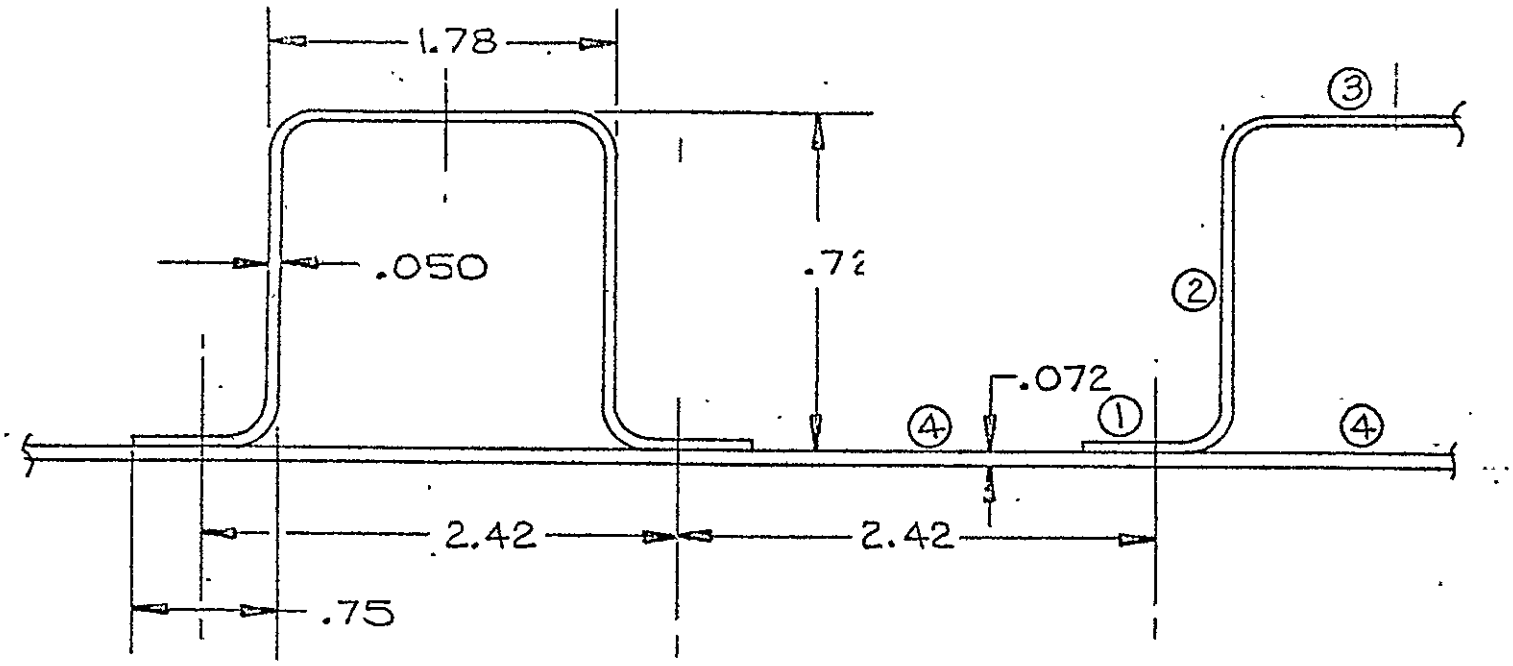

APPLIED ULT. LOAD ~ COMPRESSION = 851.45 LBS/IN
SHEAR. = 338.0 LBS/IN

EFF A = .1400 IN^2/IN WEIGHT = .00924 LBS/IN ARC & LENGTH

APPLIED COMPRESSION STRESS 6,016 LBS/IN^2

ALLOWABLE COMPRESSION CRIPPLING STRESSES	①~	21,969 LBS/IN^2
	②~	9,539 " "
	③~	9,000 " "
	④~	9,000 " "
ALLOWABLE COLUMN BUCKLING STRESS		6,256 LBS/IN^2
APPLIED SHEAR STRESS		4,674 LBS/IN^2
CRITICAL SHEAR STRESS		4,698 LBS/IN^2 (STIFFENER CRITICAL)

NOTE: ALL LOADS & STRESSES ARE ULTIMATE.

FIBERGLASS HAT SECTION

FIGURE 5

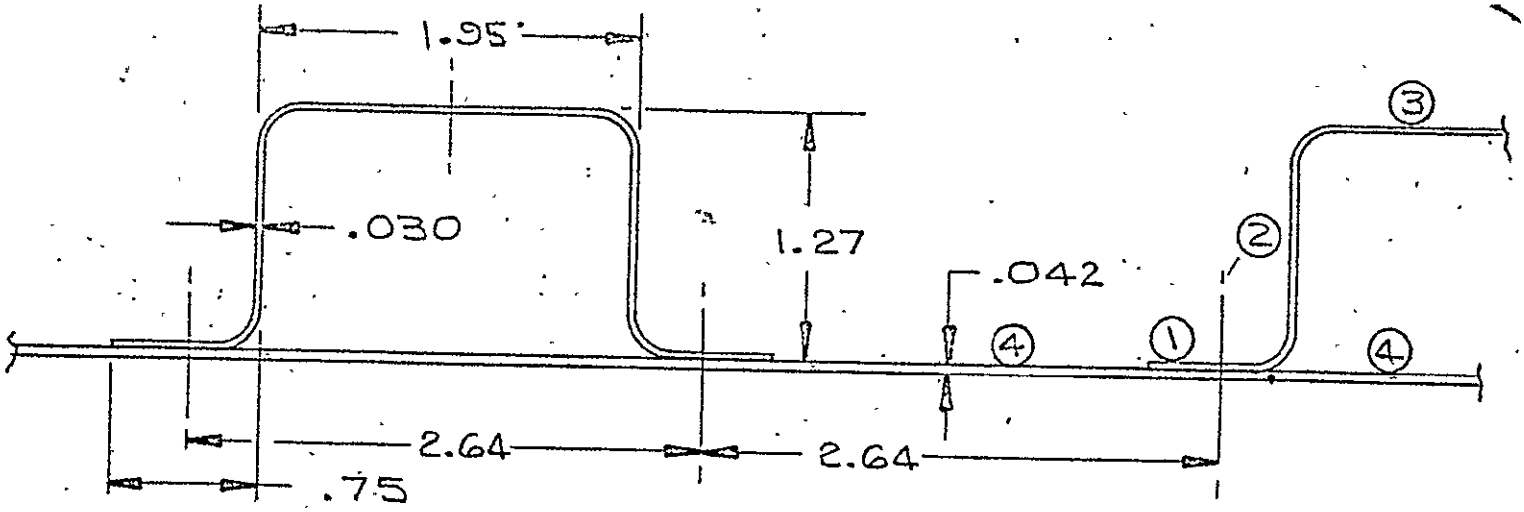

APPLIED ULT. LOAD COMPRESSION = 851.45 LBS/IN
SHEAR = 338.0 LBS/IN

EFF. A. = .0725 IN^2/IN WEIGHT = .0116 LBS/IN CIRC. & LENGTH

APPLIED COMPRESSION STRESS = 11,306 LBS/IN^2

ALLOWABLE COMPRESSION CRIPPLING STRESSES	①	44,262 LBS/IN^2
	②	36,446 " "
	③	15,000 " "
	④	15,000 " "

ALLOWABLE COLUMN BUCKLING STRESS } 19,063 LBS/IN^2

APPLIED SHEAR STRESS } $338/.030$ = 11,270 LBS/IN^2.

CRITICAL SHEAR STRESS } = 11,721 LBS/IN^2 (STIFFENER CRITICAL)

NOTE: ALL LOADS AND STRESSES ARE ULTIMATE

TITANIUM HAT SECTION

FIGURE 6

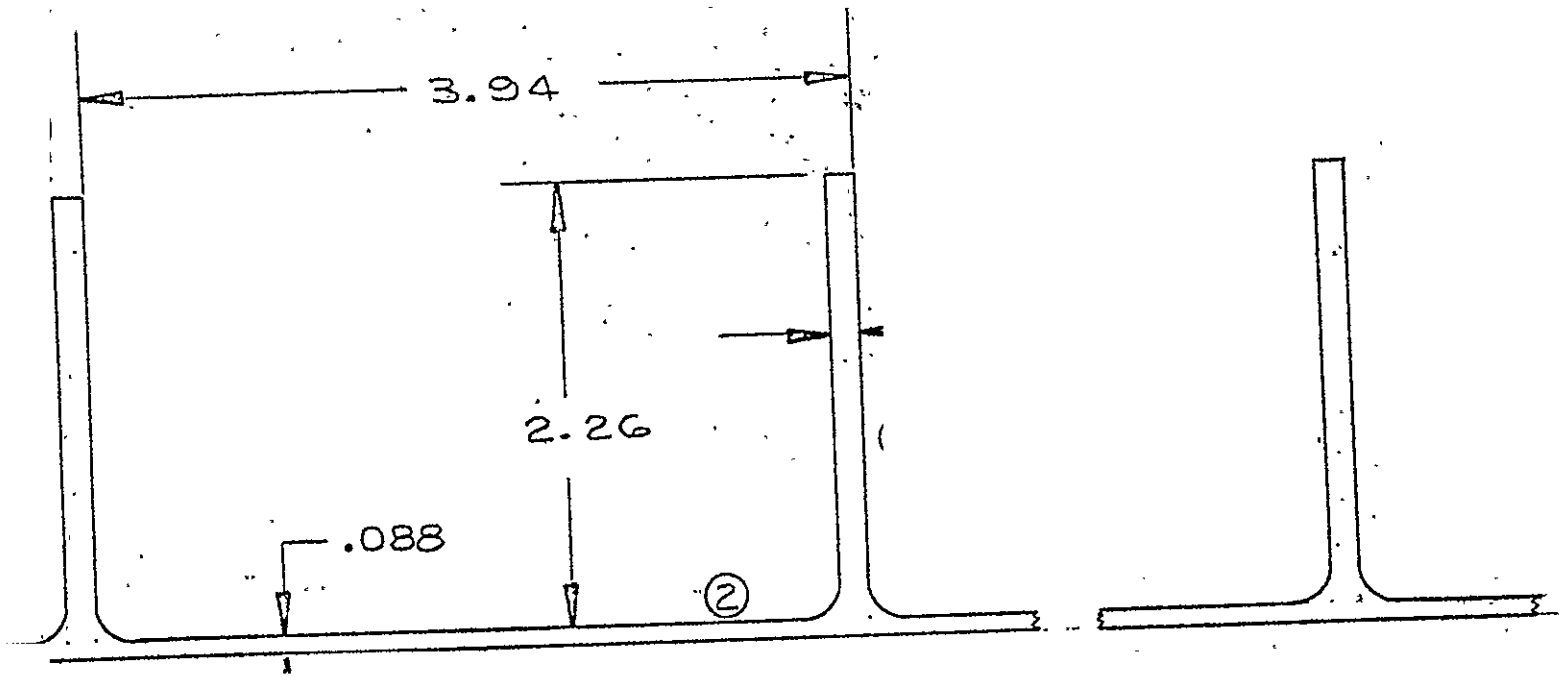

APPLIED ULT LOADS: COMPRESSION = 851.45 LBS/IN
SHEAR = 338.00 " "

EFF: AREA = .176 IN^2/IN WEIGHT = .0116 LBS/IN CIRCUM & LENGTH

APPLIED COMPRESSION STRESS	=	4,829 LBS/IN^2
ALLOWABLE CRIPPLING COMPRESSION STRESS ① & ②	=	5,000 " "
ALLOWABLE COLUMN BUCKLING STRESS	=	4,933 " "
APPLIED SHEAR STRESS	=	2,195 " "
CRITICAL SHEAR STRESS	=	4,482 " "

FIBERGLASS BAR STIFFENED PANEL

FIGURE 7

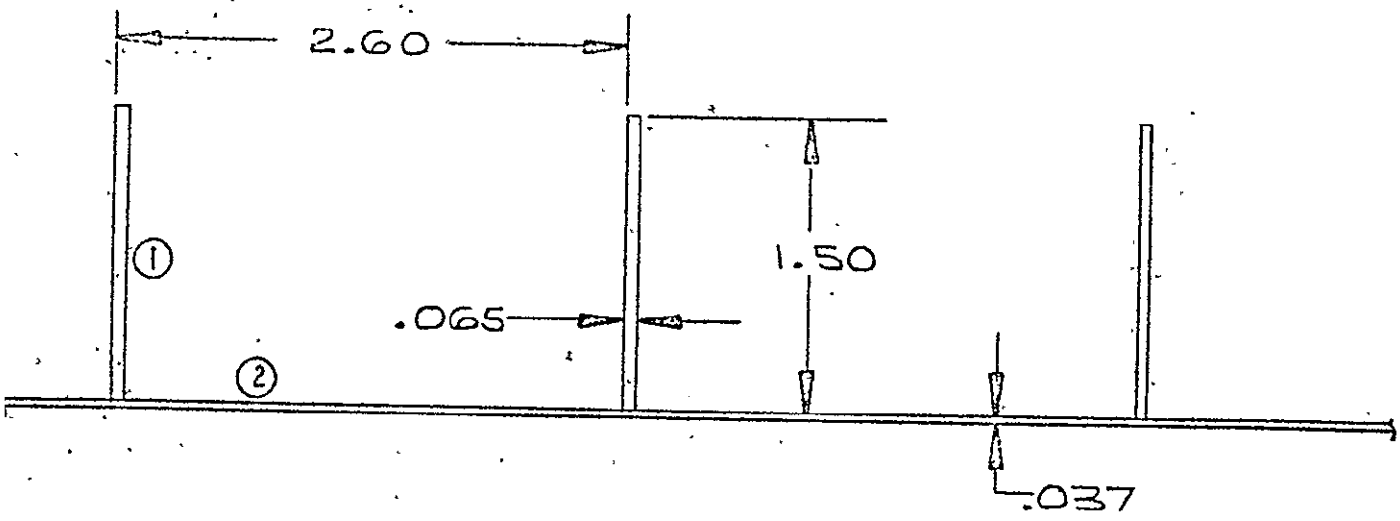

APPLIED ULT LOADS: COMPRESSION = 851.45 LBS/IN
SHEAR = 338.00 " "

EFF AREA=.0744 IN^2/IN WEIGHT = .0119 LBS/IN CIRCUM & LENGTH

APPLIED COMPRESSION STRESS	=	11,438 LBS/IN^2
ALLOWABLE CRIPPLING COMPRESSION STRESS ① & ②	=	12,000 LBS/IN^2
ALLOWABLE COLUMN BUCKLING STRESS	=	11,529 LBS/IN^2
APPLIED SHEAR STRESS	=	4,543 LBS/IN^2
CRITICAL SHEAR STRESS	=	7,042 LBS/IN^2

TITANIUM BAR STIFFENED PANEL

FIGURE 8

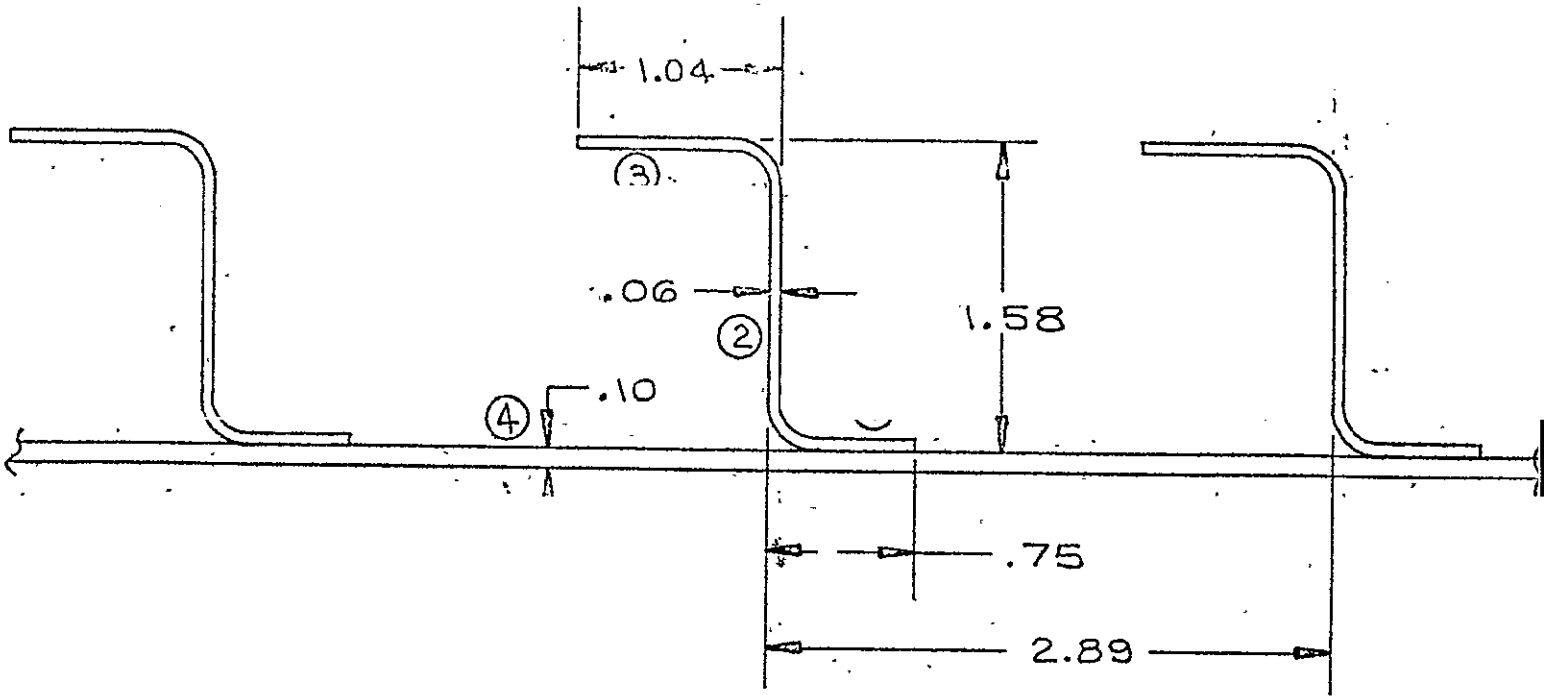

APPLIED ULT LOAD ~ COMPRESSION = 851.45 LBS/IN
SHEAR = 338.0 LBS/IN

EFF A = .1675 IN^2/IN WEIGHT = .011.1 LBS/IN CIRC LENGTH

APPLIED COMPRESSION STRESS = 5,083 LBS/IN^2

ALLOWABLE COMPRESSION CRIPPLING STRESSES
① ~ 31,000 LBS/IN^2
② ~ 16,912 " "
③ ~ 12,000 " "
④ ~ 12,000 " "

ALLOWABLE COLUMN BUCKLING STRESS = 5,118 LBS/IN^2

APPLIED SHEAR STRESS = 5,633 LBS/IN^2

CRITICAL SHEAR STRESS = 8,132 LBS/IN^2 (STIFFENER CRITICAL)

NOTE: ALL LOADS & STRESSES ARE ULTIMATE

FIBERGLASS ZEE SECTION

FIGURE 9

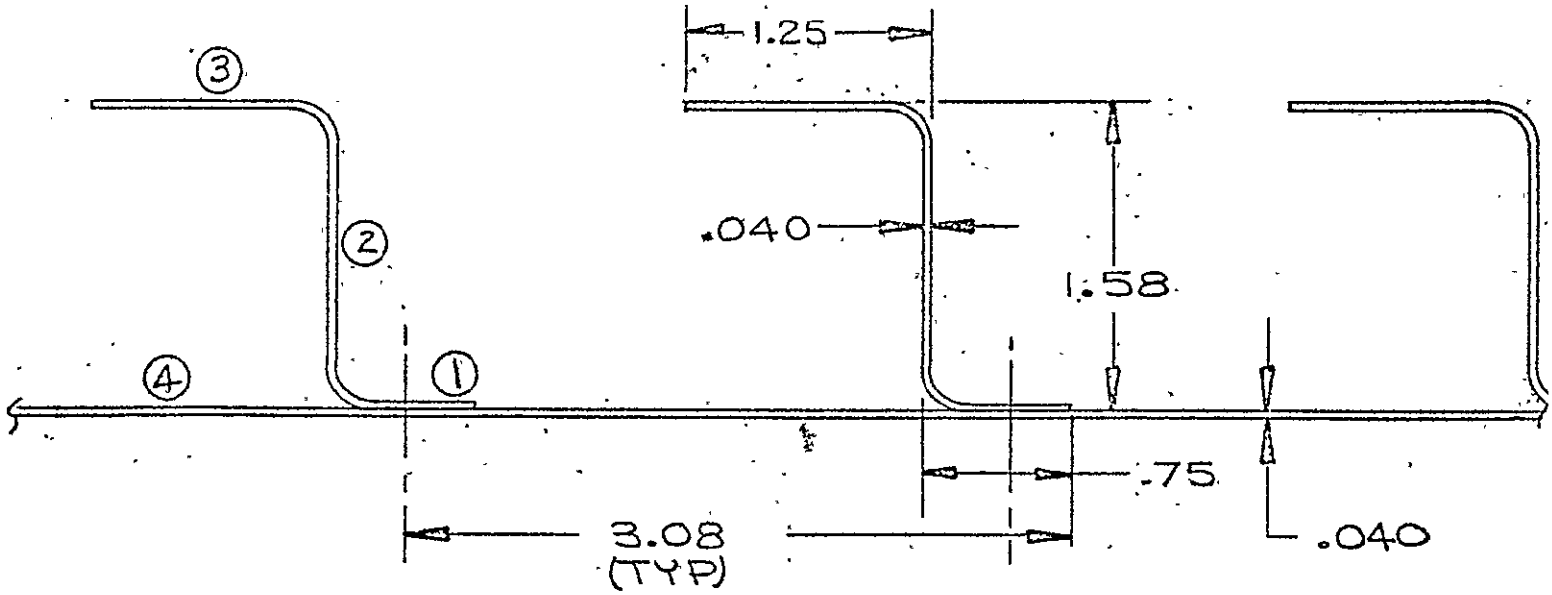

APPLIED ULT LOAD ~ COMPRESSION = 851.45 LBS/IN
SHEAR = 338.0 LBS/IN.

EFF A = .0855 IN^2/IN WEIGHT = .0137 LBS/IN CIRCUM & LENGTH

APPLIED COMPRESSION STRESS = 9,958 LBS/IN^2

ALLOWABLE COMPRESSION CRIPPLING STRESSES
- ① ~ 80,920 LBS/IN^2
- ② ~ 42,162 " "
- ③ ~ 21,200 " "
- ④ ~ 10,000 " "

ALLOWABLE COLUMN BUCKLING STRESS } 9,958 LBS/IN^2 (TORSIONAL INSTABILITY)

APPLIED SHEAR STRESS } 8,450 LBS/IN^2

CRITICAL SHEAR STRESS } 9,258 LBS/IN^2 (STIFFENER CRITICAL)

NOTE: ALL LOADS & STRESSES ARE ULTIMATE

TITANIUM ZEE SECTION

FIGURE 10

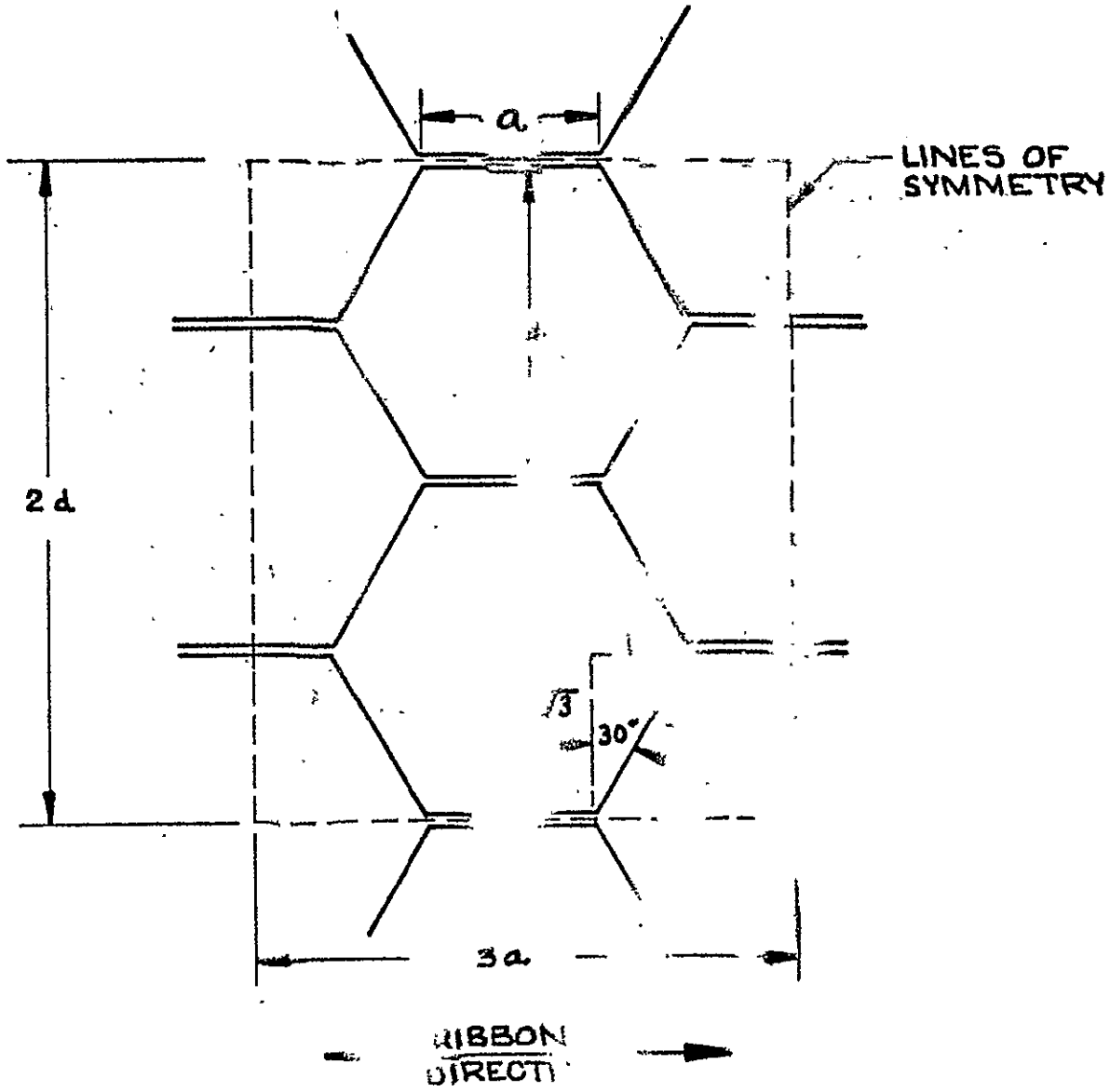

d : CEL SIZE

a : SID OF CELL

a : d/2 COS 30° d/√3

FIGURE 11

Using developed length

$$\text{Core heat flow} = \frac{K_c \times \rho_c \times T_c}{4608\ \rho_f}$$

where K_c = mean thermal conductivity of the core

ρ_c = density of the core

T_c = core thickness

ρ_f = density of the foil

Several different methods utilizing different theories were available for the design of sandwich cylinders subjected to axial compression or bending loads which could cause buckling. One method, MIL-HDBK-23 (Reference 15), used a large deflection theory and established the minimum postbuckling load of the theoretical load-shortening curve of sandwich cylinders as the design load of the cylinders; thus, it could not be expected to predict the buckling load. This had been the most commonly used method in design but the method was found to be quite conservative, e.g., Reference 16.

A second method made use of small-deflection classical buckling theory which differed from ordinary curved-plate theory principally by the inclusion of the effects of deflections due to transverse shear. This theory was modified, when necessary, to account for the fact that cylinders do not always sustain the classical buckling load prior to buckling. However, the modification was slight when compared to monocoque shells. This method yielded buckling loads that could be as high as 2 1/2 times that of the first method. The principal problem encountered in applying this method to design was the lack of sufficient experimental data to substantiate the method. Equations for the application of this method were taken from Reference 17.

A third method made use of an effective moduli of elasticity and thickness of the sandwich shell as described in Reference 18. The values of E_e and T_e

can be substituted into the formulas for solid isotropic shells or plates. These effective values are

$$E_e = \frac{H}{2\sqrt{3\,(1-\mu^2)\,D/H}} = \text{Effective modulus of elasticity}$$

$$T_e = 2\sqrt{3\,(1-\mu^2)\,D/H} = \text{Effective thickness}$$

where μ = Poisson's ratio of the face material

$H = E_f\,(t - t_c)$ (Extensional Stiffness)

t is the overall thickness of the honeycomb panel and t_c is the core thickness and E_f = modulus of elasticity of face material.

$D = E_f\,(t^3 - t_c^3)/12\,(1-\mu^2)$ (Bending Stiffness)

The values obtained for critical buckling loads and deflections by this substitution are always unconservative, due to shear deflections.

Conservative values of critical buckling loads per inch of panel edge were obtained by:

$$P_{cr} = \frac{1}{\frac{1}{P_{cre}} + \frac{1}{U}}$$

$U = 1/2\,(t + t_c)$ G_c = transverse shear stiffness

G_c = core shear modulus $\sim$ lbs/in^2

in which P_{cr} is a conservative value of the critical load per inch of panel edge, P_{cre} is the unconservative value obtained by substituting E_e and T_e in a formula for solid isotropic plates.

For this method the equations for isotropic monocoque shells that are based

on considerable experimental data and presented in Reference 19 were used. These were:

$$P_{cr} = C\ 2\ \pi\ E\ T^2$$

$$F_{cr} = C\ E\ \frac{T}{R}$$

C = Buckling Coefficient

$$C = .606 - .546\left\{1.0 - \exp.\left[-\frac{1}{16}\ (R/T)^{1/2}\right]\right\} + .9\ (R/L)^2\ (T/R)$$

where T and E can be replaced by T_e and E_e.

A fourth method also made use of the effective moduli of elasticity and thickness of the honeycomb sandwich shell wall as described in Reference 18. A one inch strip of the shell was treated as an Euler column.

It was shown that the buckling of this conical support would always occur in only 1/2 of a longitudinal wave (axisymmetric mode), therefore, this method of analysis was applicable. This approach was considered to be quite conservative since no effect of curvature or hoop stiffness was included. The Euler column load was reduced for the effect of shear deflection of the core material. This method yielded allowable loads which were intermediate to the other methods and was chosen for final design.

The final design equation became:

$$P_{cr} = \frac{\pi^2\ D}{L^2 + \frac{\pi^2\ D}{U}}$$

where D was the bending stiffness and U was the shear stiffness as previously defined.

A comparison of the various analysis methods is shown in Figure 12. This comparison is for a representative fiberglass honeycomb cylinder tank support using .036 inch face skins and 2 inch core for a length of 45.47 inches. It is shown that the analysis method chosen is conservative.

OPTIMIZATION PROCEDURE

The optimization was performed with a digital computer using an iterative procedure.

The honeycomb sandwich was checked for intracell buckling, face wrinkling, and shear crimping in addition to the overall shell buckling that was discussed in the previous section. The equations for the first three failure modes listed are as follows:

Intracell compression buckling stress (Reference 18)

$$F_{cib} = 2E\,(t_f/cell)^2$$

where t_f = face skin thickness - in.

cell = cell size - in.

Face wrinkling stress (Reference 17)

$$F_{cw} = .43\,(E \times E_{core} \times G_{core})^{1/3}$$

where E_{core} = Core compression modulus of elasticity - lbs/in^2

G_{core} = Core shear modulus of elasticity - lbs/in^2

Face shear crimping stress due to compression loads (Reference 17)

$$F_{csc} = \frac{G_{core}\,(t_c + 2\,t_f)}{2\,t_f}$$

where t_c = core thickness - in.

t_f = face skin thickness - in.

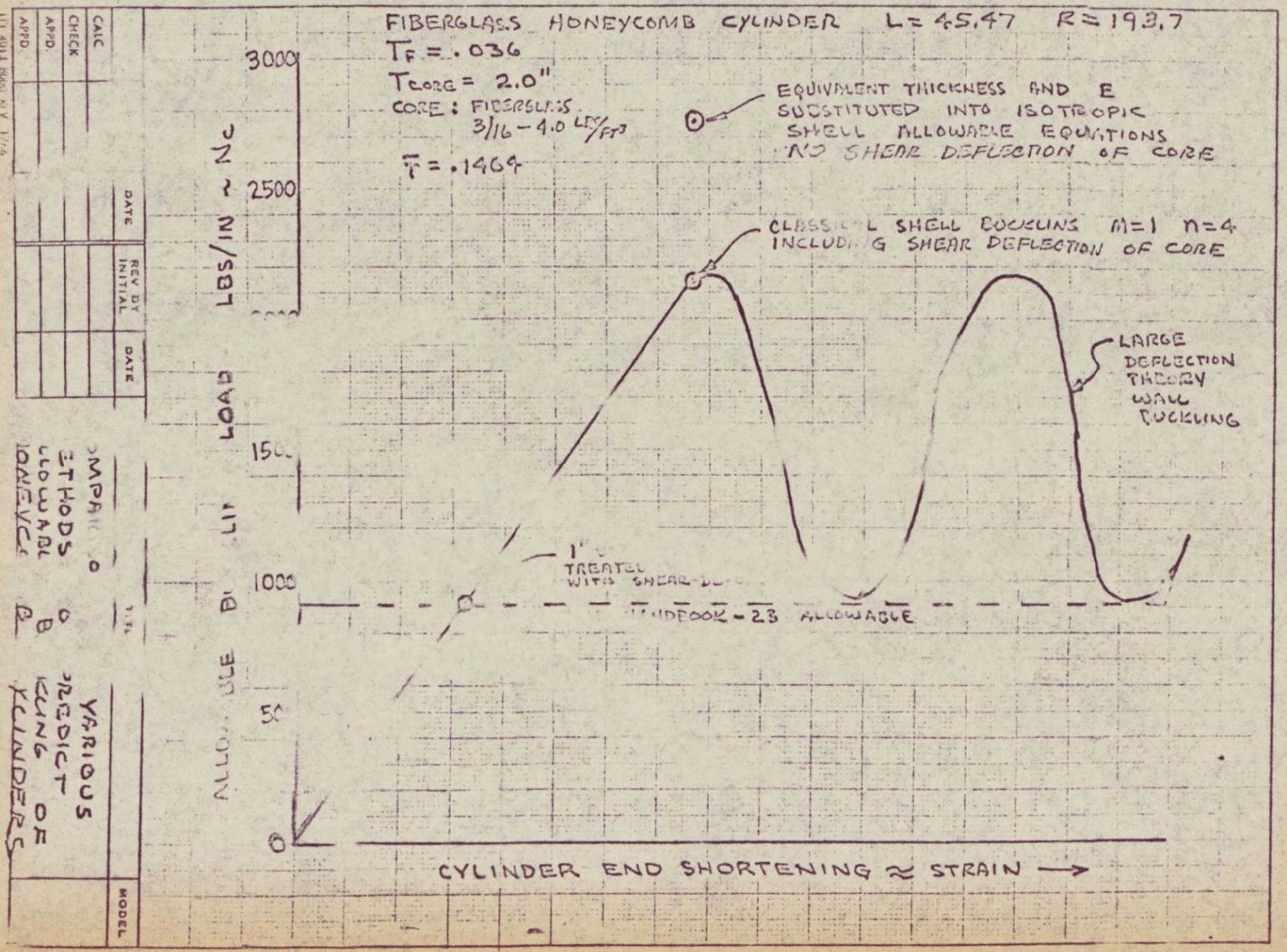

CALC					
CHECK					
APPD.					
APPD.					

DATE	REV BY INITIAL	DATE

REV LTR

40

COMPARISON OF ETHODS ALLOWABLE LOADS

VARIOUS PREDICT BUCKLING OF CYLINDERS

MODEL

FIGURE 12

The configuration which fulfilled these requirements and provided minimum cross sectional area was considered optimum.

Face thicknesses in increments of .009 inches were considered for fiberglass. Minimum gage for the titanium was .005 inches and increments of .001 inches were considered. Standard sizes of fiberglass honeycomb core were used.

The design loading was 878 lbs/inch which occurred at the bottom of the support and was the critical condition since tapering of the honeycomb construction was not considered.

RESULTS

The optimization results for both fiberglass and titanium sandwich cone supports are tabulated in Figures 13 and 14. It can be seen that optimum weight and heat flow did not occur with one configuration, thus a compromise was necessary. Figures 15 and 16 show the configurations selected. The all fiberglass configuration was only slightly "off optimum" in heat flow and was narrower, which minimized clearance problems between cone support and tank head. The titanium configuration selected was the one with minimum heat flow. This was necessary to make the concept competitive with fiberglass construction. The weight difference between fiberglass and titanium construction was negligible; however, the cross sectional area of the titanium member was significantly less.

2.4.4 Weight-Heat Flow Comparisons

Figure 17 lists the results of the study. It should be noted that the values are for one inch of cone circumference and, therefore, do not represent total heat flow or weight. Also the weight and heat flow additions due to edge attachments are not included. A comparison of results shows fiberglass construction to be superior for like configurations both on a weight and heat flow

	FACE THK IN.	FIBERGLASS CORE THK IN.	HEX CELL SIZE	DENSITY LBS/FT³	$\overline{T}$ EFF THK	KA/IN BTU-IN / HR-°F ×10⁻³	WEIGHT LBS/IN²
	.036	2.0	3/8	2.2	.1232	1.15 (1.12)	.0081
	.036	2.1	3/8	2.2	.1251	1.16 (1.13)	.0083
	.027	2.2	1/4	3.5	.1341	1.08 (1.03)	.0089
OPT. WT.	.027	2.3	3/8	2.2	.1109	0.95 (.92)	.0073
	.027	2.4	3/8	2.2	.1129	0.96 (.93)	.0075
	.027	2.5	3/8	2.2	.1148	0.97 (.94)	.0076
	.027	2.6	3/8	2.2	.1168	0.98 (.95)	.0077
OPT. Q	.018	2.7	1/4	3.5	.1315	0.93 (.87)	.0087
	.018	2.8	1/4	3.5	.1345	0.95 (.89)	.0087
	.018	2.9	1/4	3.5	.1376	0.97 (.90)	.0091
	.018	3.0	1/4	3.5	.1407	0.99 (.92)	.0093
	.018	3.1	1/4	3.5	.1437	1.00 (.93)	.0095
	.018	3.2	1/4	3.5	.1468	1.02 (.95)	.0097
	.018	3.3	1/4	3.5	.1499	1.04 (.96)	.0099
	.018	3.4	1/4	3.5	.1530	1.06 (.98)	.0101
	.018	3.5	1/4	3.5	.1560	1.07 (.99)	.0103
	.018	3.6	1/4	3.5	.1591	1.09 (1.01)	.0103
	.027 .018	3.7 3.7	3/8 1/4	2.2 3.5	.1380 .1623	1.10 (1.02)	.0091
	.027	3.8	3/8 1/4	2.2 3.5	.1399 .1652	1.11 (1.04)	.0092
	.027 .018	3.9	3/8 1/4	2.2 3.5	.1418 .1683	1.13 (1.05)	.0094

	INITIALS	DATE	REV BY INITIALS	DATE	TITLE	MODEL
CALC		7-11-68			HONEYCOMB CONSTRUCTION FIBERGLASS	
CHECK						
APPD.						
APPD						

* NUMBERS IN PARENTHESIS ARE FOR DEVELOPED CORE LENGTH.

BOEING NO

FIGURE 13

	FACE THK IN.	FIBERGLASS CORE			T EFF THK	KA/IN BTU-IN / HR-°F x10⁻³	WEIGHT LBS/IN³
		THK IN.	HEX CELL SIZE	DENSITY LBS/FT³			
	.022	1.0	3/16	4.0	.0637	10.76 (10.73)	.0102
	.018	1.1	3/16	4.0	.0571	8.86 (8.83)	.0091
	.015	1.2	3/16	4.0	.0526	7.44 (7.41)	.0084
	.013	1.3	3/16	4.0	.0500	6.50 (6.46)	.0080
	.011	1.4	3/16	4.0	.0475	5.56 (5.52)	.0076
OPT WT	.010	1.5	1/4	3.5	.0442	5.06 (5.02)	.0071
	.009	1.6	3/16	4.0	.0464	4.64 (4.59)	.0074
OPT Q	.008	1.7	3/16	4.0	.0458	4.18 (4.13)	.0073
	.008	1.8	3/16	4.0	.0472	4.20 (4.15)	.0076
	.008	1.9	3/16	4.0	.0487	4.21 (4.16)	.0078
	.008	2.0	3/16	4.0	.0501	4.23 (4.18)	.0080
	.009	2.1	3/16	4.0	.0515	4.25 (4.20)	.0082
	.008	2.2	3/16	4.0	.0530	4.27 (4.22)	.0085
	.008	2.3	3/16	4.0	.0545	4.29 (4.23)	.0087
	.008	2.4	3/16	4.0	.0559	4.31 (4.25)	.0089
	.008	2.5	3/16	4.0	.0574	4.33 (4.27)	.0092
	.008	2.6	3/16	4.0	.0588	4.35 (4.28)	.0094
	.008	2.7	3/16	4.0	.0603	4.37 (4.30)	.0096
	.008	2.8	3/16	4.0	.0617	4.39 (4.32)	.0099
	.008	2.9	3/16	4.0	.0632	4.41 (4.34)	.0100

	INITIALS	DATE	REV BY INITIALS	DATE	TITLE	MODEL
CALC		7-12-8			HONEYCOMB CONSTRUCTION TITANIUM	
CHECK						
APPD.						
APPD						

* NUMBERS IN PARENTHESIS ARE FOR DIVERGENT CORE LENGTH.

REV LTR

BOEING NO

SH. FIGURE 14

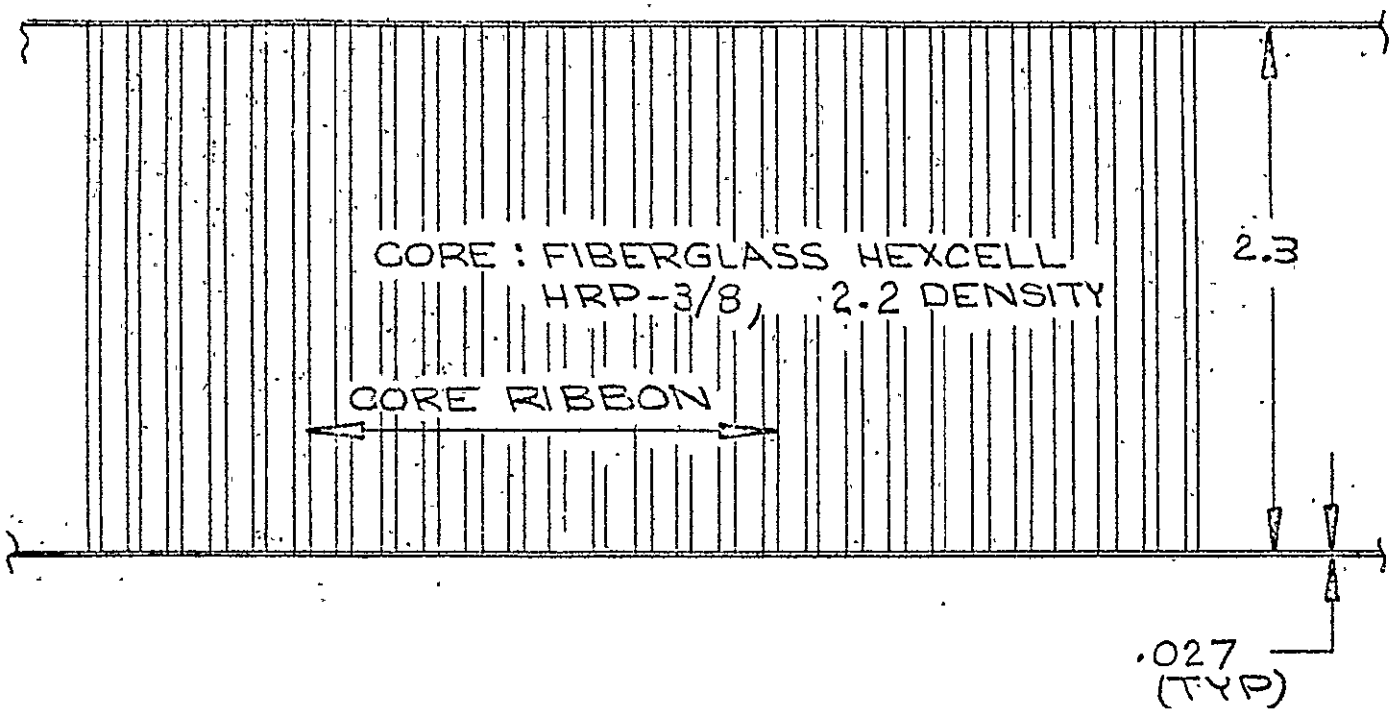

APPLIED ULT. LOAD ~ COMPRESSION = 878.06 LBS/IN
SHEAR = 338.00 " "

EFF AREA = .1109 IN²/IN WEIGHT = .0073 LBS/IN-CIRCUM & LENGTH

APPLIED ULT COMPRESSION STRESS =	24,391	LBS/IN²
ALLOWABLE COMPRESSION BUCKLING STRESS =	25,503	" "
ALLOWABLE COMPRESSION INTRACELL BUCKLING STRESS =	31,104	" "
ALLOWABLE COMPRESSION FACE WRINKLING STRESS =	52,435	" "
ALLOWABLE COMPRESSION SHEAR CRIMPING STRESS =	516,800	" "

HONEYCOMB, FIBERGLASS FIBERGLASS FACES

FIGURE 15

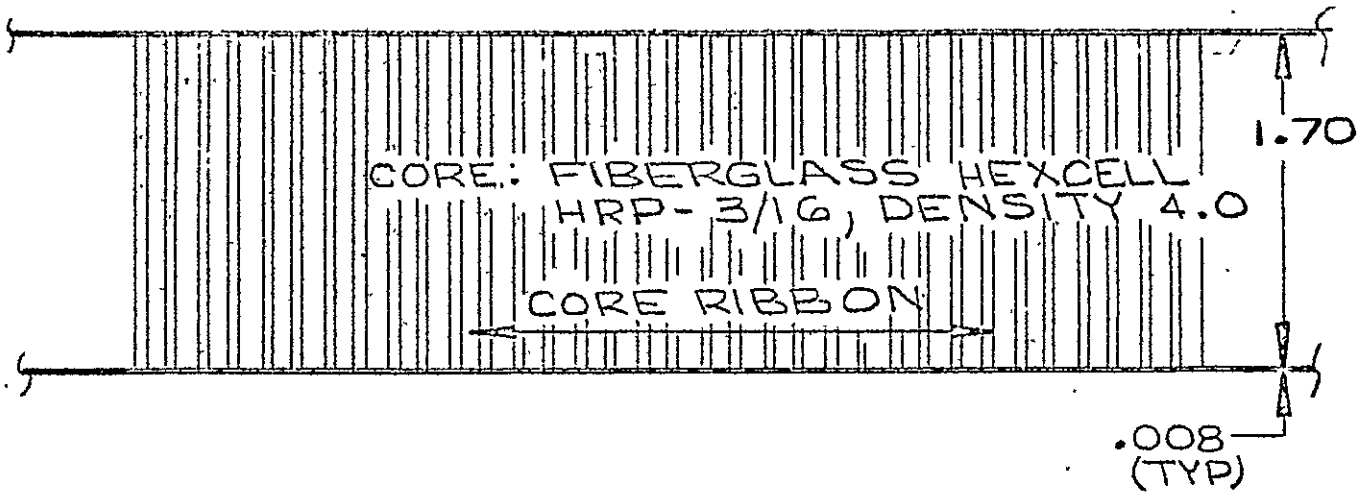

APPLIED ULT. LOAD ~ COMPRESSION = 878.06 LBS/IN
SHEAR = 338.00 " "

EFF. A. = .0458 IN²/IN, WEIGHT = .0073 LBS/IN CIRCUM & LENGTH

APPLIED ULT COMPRESSION STRESS	=	54,879 LBS/IN².
ALLOWABLE COMPRESSION BUCKLING STRESS	=	59,641 " "
ALLOWABLE COMPRESSION INTRACELL BUCKLING STRESS	=	59711 " "
ALLOWABLE COMPRESSION FACE WRINKLING STRESS	=	201,240 " "
ALLOWABLE COMPRESSION SHEAR CRIMPING STRESS	=	1,211,925 " "

HONEYCOMB FIBERGLASS TITANIUM FACE'S

FIGURE 16

CONSTRUCTION	FIBERGLASS				TITANIUM			
	EQUIV. AREA / INCH-CIRCUM (IN^2/IN)	WEIGHT / INCH-CIRCUM & INCH-LENGTH (LBS/IN^2)	HEAT FLOW / INCH-CIRCUM & INCH-LENGTH (BTU/HR)	WEIGHT-HEAT FLOW PRODUCT $\times 10^{-3}$	EQUIV. AREA / INCH-CIRCUM (IN^2/IN)	WEIGHT / INCH-CIRCUM & INCH-LENGTH LBS/IN^2	HEAT FLOW / INCH-CIRCUM & INCH LENGTH	WEIGHT HEAT / FLOW PRODUCT $*10^{-3}$
CORRUGATION	.092	.0061	.60	3.7	.041	.0066	4.96	32.7
HONEYCOMB	.111	.0073	.48	3.5	.046	0073	2.09	15.3
HAT STIFFENER	.140	.0092	.91	8.4	.073	.0116	8.75	101.5
ZEE STIFFENER	.168	.0111	1.09	12.1	.086	.0137	10.31	141.5
BAR STIFFENER	.176	.0116	1.15	13.4	.074	.0119	8.87	105.5

FIGURE 17

HEAT FLOW VALUES ASSUME THAT PART IS SUFFICIENTLY LONG TO YIELD EQUILIBRIUM TEMPERATURES OF -423°F & +80°F AT COLD & WARM ENDS RESPECTIVELY AND HEAT FLOW IS ONE DIMENSIONAL WITHOUT INSULATION INTERACTION.

LOAD $N_c = .851$ LBS/IN
$\Delta T = 500°F$

TITANIUM MEAN THERMAL CONDUCTIVITY = $0.24 \frac{BTU - IN}{IN^2 - HR - °F}$
FIBERGLASS " " " $= 0.013$

basis. The weight-heat flow parameter differences were largely the effect of the fiberglass thermal conductivity, pointing out the main advantage of this material.

Fiberglass honeycomb sandwich was the best choice of materials in this comparison chart with fiberglass corrugations a close second choice. The most promising titanium construction method yielded a heat flow 4 times greater for approximately equivalent weight.

Figure 18 shows weight trends for various construction methods as the compression loading was increased. The figure shows that the zee and bar stiffened panels were the heaviest. This was due largely to the conservative torsional instability analysis employed. The titanium zee was less efficient than the fiberglass zee because of the same lack of torsional stiffness in thin gages. The other forms of construction were not subject to this mode of failure. The requirements of (1) critical local shear stability of the skin, and (2) stiffener moment of inertia for modes of general instability in shear, showed major effects on all the stiffened types of construction. These effects gave fiberglass a weight advantage over titanium because local shear buckling of the skin is a function of Et^2 in the elastic range, e.g., for the equal weight stiffeners of fiberglass and titanium shown in the sketch below, the moment of inertia of the fiberglass is greatest as is Et^2.

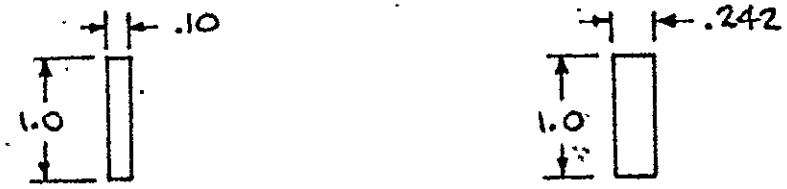

Titanium Fiberglass

Et^2 (fiberglass) = $3.0 \times 10^6 (.242)^2 = 17.6 \times 10^4$

Et^2 (titanium) = $16.4 \times 10^6 (.10)^2 = 16.4 \times 10^4$

For the honeycomb sandwich analysis, the fiberglass face skins were restricted

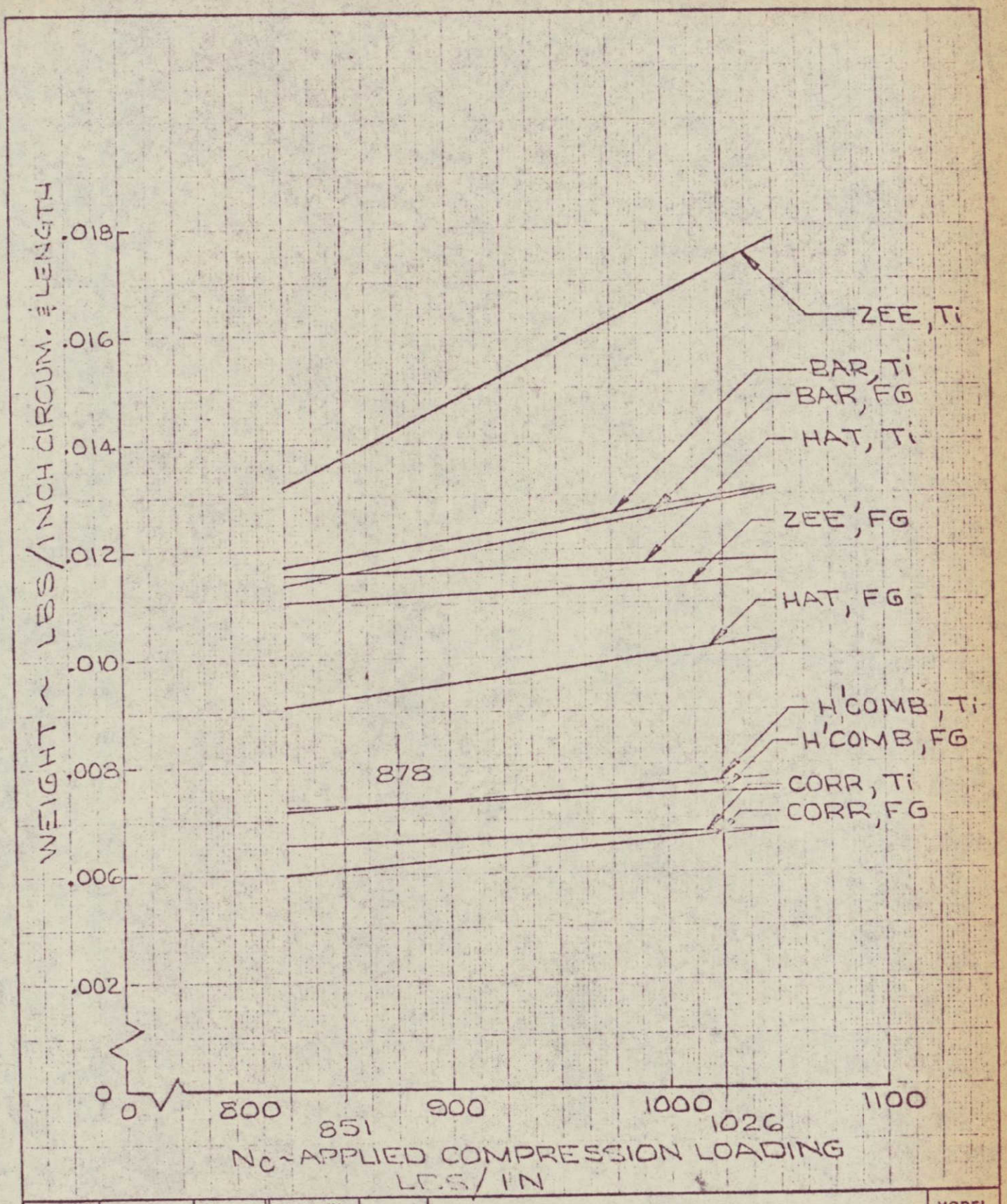

	INITIALS	DATE	REV BY INITIAL	DATE	TITLE	MODEL
CALC						
CHECK						
APPD.						
APPD.						

to .009 inches or increments thereof, while the titanium skins were allowed to vary in increments of .001 inch. This caused the cross over of the weight curves. The corrugated construction did not employ any gage limitations and is more indicative of actual material capabilities, i.e., fiberglass has weight advantages for lower loads and titanium for higher loads.

2.5 Structural Concept Designs

Detail designs were developed for each structural concept studied. The designs were prepared and analyzed in sufficient detail to allow realistic weight estimation. The designs are presented in Figures 19 through 26.

It was assumed that the cone would become a semi-permanent part of the tank assembly and, therefore, blind fasteners could be used in limited access areas such as the cone to tank joint. However, it was believed necessary to maintain disassembly capability at the forward attachment to stage structure.

The skin stiffened designs of Figures 24, 25, and 26 all involved the use of somewhat complex end attachment fittings. The fittings were believed necessary to assure a uniform stress distribution across skin and stiffener, which was assumed to be the case in the computer structural optimization studies. The method of fabricating the bar stiffened titanium construction was not explored in detail and instead the welded concept proposed by other investigators was assumed. The welded configuration may in reality be difficult to manufacture and maintain straightness in the thin gages.

The corrugated designs show two approaches to end attachment. The inner and outer ring designs of Figures 19 and 21 require that the load concentration at the fasteners be dissipated into all surfaces of the corrugation. An improvement of this approach is shown in Figures 20 and 22 where all surfaces of the corrugation are attached providing a more uniform load transfer across

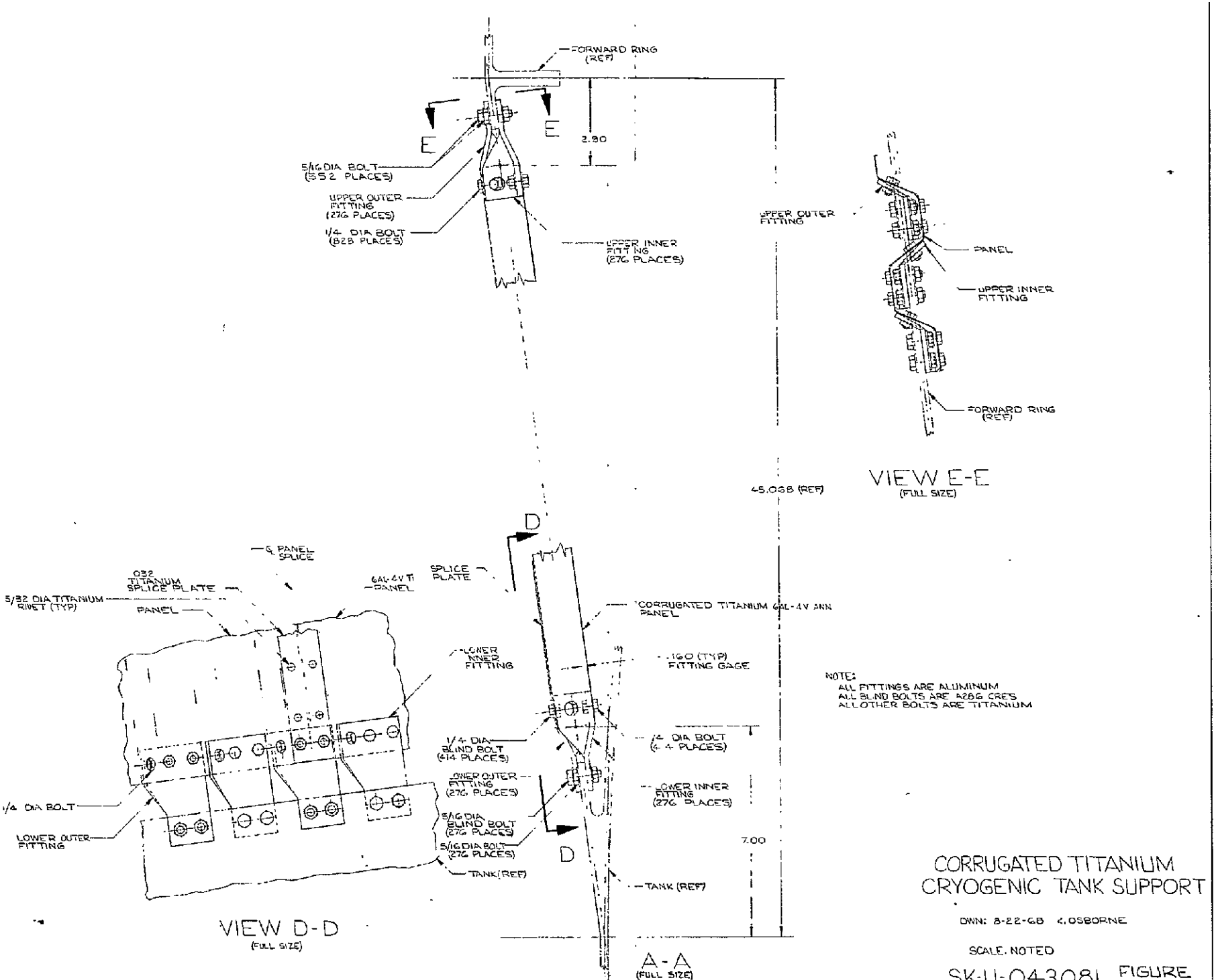

ALTERNATE ATTACHMENT

CORRUGATED TITANIUM CRYOGENIC TANK SUPPORT

DWN: 8-22-68 K. OSBORNE

SCALE: NOTED

SK-11-043081 FIGURE 20

SHEET 2 OF 2

the joint. This latter configuration requires fabrication of a large quantity of complex plates.

The honeycomb sandwich with the "in plane" attachment leg provides the simplest attachment scheme since complex formed metal parts are eliminated. This concept can also be manufactured in a minimum number of segments because the bonded structure is light weight and rigid providing ease of handling for subsequent assembly stages.

An analysis of thermal stresses was made. The approach taken was to consider the area ratios of "hot" and "cold" members, A_h and A_c. These ratios, in conjunction with Young's modulus, E, and coefficient of expansion α, were used for preliminary evaluations of material and material combinations under thermal gradients. The approach is illustrated in Figure 27. The ordinate is the stress in an element at -423°F. The abscissa is the stress in an element at 70°F. An initial temperature of 70°F was assumed for both elements. The values of thermal stress were determined by the equations:

$$\sigma_{T_c} = - \frac{E_c \left[\alpha_c \Delta T_c - \alpha_h \Delta T_h \right]}{\frac{E_c A_c}{E_h A_h} + 1}$$

$$\sigma_{T_h} = - \frac{E_h \left[\alpha_h \Delta T_h - \alpha_c \Delta T_c \right]}{\frac{E_h A_h}{E_c A_c} + 1}$$

where T_h and T_c represent temperatures of hot and cold members respectively.

Various values of the ratio A_c/A_h were calculated and plotted so that the stresses at any area ratio could be read for both hot and cold members.

From this figure, the materials and combinations of materials which alleviated

SHEET 65

FIGURE 27

the effects of thermal gradients could be determined. It is important to note that not only the magnitude of the thermal stress was important, but also the slope of the line for the designated materials. For this study the adjoining members, i.e., the cone support and tank "y" ring were assumed to be at opposite temperature extremes. Selecting the most critical condition for the cone, where $A_c/A_h = \infty$, it can be seen that the titanium cone would incur significantly higher stresses than the fiberglass cone. The maximum thermal hoop compression stresses that could be generated for this condition were - 12,000 psi in the fiberglass cone and - 68,000 psi in the titanium cone. This comparison showed the superiority of the fiberglass for reducing thermal stresses due to lower modulus of elasticity. The stresses produced in the fiberglass under the most severe conditions were small and the designs had adequate capacity, whereas in the titanium, the stresses were significant, indicating a possible need for translating joint designs.

Preliminary results showed a slight weight advantage for fiberglass in most of the cone configurations. Incorporation of a translating joint in the titanium cone would only have made this design heavier; therefore, the study effort to develop this type of design was considered unwarranted.

In actual applications the temperature extremes would probably not exist for long and any deflections resulting from thermal gradients would tend to reduce thermal stresses.

2.5.1. Manufacturing Feasibility

SK 11-043081 - Corrugated Titanium (Figures 19 and 20)

Forming of corrugations would present an extremely difficult problem because the corrugation shape is tapered. The job could probably be accomplished best in heated, matched metal forming dies; however, development would be necessary.

Heated forming (1200°F) of titanium would require application of a protective finish to avoid surface oxidation with the attendant cleaning problems. The number of formed cone segments would be a function of sheet width availability and forming technique. Segment joints would be used to provide circumferential "pay-off" for matching with the tank "y" ring.

Forming of the "y" shaped tank attach rings would take some development. An approach would be to make matched metal forming dies with the required curvature. This would permit fabrication of only relatively short lengths, therefore, a great quantity of parts would be necessary. Stretch forming is a candidate process, and except for die costs, would be relatively inexpensive. Roll forming to shape and curvature on Yoder Rolls is also a possibility.

Figure 20 shows forged attach plates instead of formed rings. The plates would require fabrication of two sets of forging dies (for right and left hand parts). The dies would be expensive to develop; however, the great quantity of parts would offset this cost. Corrugation shape was designed so that the same attach plates could be used at top and bottom of the cone.

SK 11-043080 - Corrugated Fiberglass (Figures 21 and 22)

Fiberglass tooling for laminating corrugated sections would be complex due to the varying corrugation width. However, once the tool was perfected, the layup and curing of laminates would be routine. Producing build-ups at the ends of corrugations would require recesses in the tool and it would be difficult to control build-up thickness without a post cure grinding operation involving hand work.

Splice joints between segments could be simplified by using bonds with only a few rivets to hold the parts in place and to apply bonding pressure. Doublers could also be bonded to cone attachment rings to minimize the number of detail

parts and to aid in positioning while drilling bolt holes. Comments regarding forming of metallic "y" attach rings and forged plates for the titanium structure apply to the fiberglass structure as well.

It was assumed in both titanium and fiberglass corrugation designs that inside "y" attachment ring segments would be bolted to the cone prior to installation on the tank. This approach would ease fit-up and the cone could then be attached to the tank using temporary fasteners. The outer attach ring segments would be added to complete the installation. Blind fasteners would be used due to limited access. In the case of forged attach plate designs, only the inner plates would be assembled to the cone prior to installation. The outer plates would be added with blind fasteners as in the case of the attach ring segments.

SK 11-043082 - Honeycomb Sandwich, Titanium Face Skins (Figure 23)

Assembly of prefabricated details by standard metalbond techniques could be accomplished with no unusual problems. Titanium skin splices would be made as material width and length dictated by lapping and adhesive bonding. The two-segment design was considered feasible in terms of tooling, curing facilities, and handling; however, scrappage of an assembly due to bonding defects or lay-up errors would be expensive because of the materials and labor involved.

Core forming did not constitute a manufacturing problem. Forming of edge attachment channels would be difficult and would require special processes such as heated, matched die forming or roll forming. Splice joint channels would be made by standard metal forming processes. The segmented "y" attach rings would present fabrication problems similar to those of the corrugated cones.

SK 11-043082 - Honeycomb Sandwich, Fiberglass Face Skins (Figure 23)

The configuration of the edge attachment laminate caused manufacturing

complications which could result in a part of questionable reliability if layup and cure of the entire assembly was made in one operation. An alternate approach would be to prefabricate laminate edge members and bond these to the core/skin assembly. This approach would necessitate additional tooling and bonding steps. Edge splice channels would be produced and installed in this manner. The outer face skin would be laminated and cured as a detail part to assure flatness. This part would be bonded to the outer surface of the core as the final process.

Assembly of panels for honeycomb sandwich designs could be accomplished separately from the tank, with the segment splice joints providing circumferential "pay-off" for fitting to the tank "y" ring. The sandwich cones were expected to be rigid and easily handled. Also, the butt joint configuration lent itself to positioning with tank and stage structure rings better than the other configurations utilizing lap joints because the part could be rested on the attachment ring. Shim stock could be used for minor fit up discrepancies. The inner splice plate could be riveted to the small end of the cone to act as a guide during assembly.

SK 11-043084 - Zee Stiffened Titanium (Figure 24)

This part did not present any unusual fabrication problems. Sheet could be formed to the required shapes using standard metal forming methods. Machined end fittings were numerous which would result in high costs. The part would be flexible and present problems in handling and assembly.

SK 11-043084 - Zee Stiffened Fiberglass (Figure 24)

This was a good design for laminated structure. Tooling and layup of the zees would be standard procedure. The reinforcements at the ends of the zees could

be built into the original layup or bonded on as a secondary step. The reinforcement at edges of the skin would be produced at the time of molding and curing. A male mold would be used. Aluminum end fittings would require extensive machining and the assemblies would be flexible and difficult to handle in large sections.

SK 11-043085 - Hat Stiffened Titanium (Figure 25)

This part could be produced using standard fabrication techniques. Hat sections could be cold formed to the required configuration. End attach fittings would require extensive milling and therefore, be costly. This part would be flexible like the zee stiffened structure.

SK 11-0430-85 - Hat Stiffened Fiberglass (Figure 25)

This design would present no unusual manufacturing problems. Comments regarding end fittings and laminate end buildups made for the zee stiffened skin are applicable.

SK 11-043086 - Bar Stiffened Titanium (Figure 26)

Welding of bars to the skin would present major manufacturing problems. EB welding from the face skin side would be possible; however, "Out of Vacuum" EB welding is mostly experimental and, if vacuum chamber welding was used, part size would be limited due to the conical shape. A great number of welding setups would be necessary due to the numerous bars, therefore labor costs would be high. Parts distortion is one of the major problems in EB welding of thin gages and it is possible that a hot sizing operation after welding this configuration would be necessary. Expensive curved dies would be required for this operation. Current manufacturing development efforts for constructing stiffened titanium panels are being directed towards diffusion bonding. This approach also requires expensive heated, matched dies, but the distortion

problem is eliminated. End fittings for the bar stiffened cone would require extensive machining.

SK 11-043086 - Bar Stiffened Fiberglass (Figure 26)

Fabrication of this concept as configured, i.e., with integral bar stiffeners, appeared to be a severe problem area. No satisfactory tooling approach was devised during the manufacturing analysis. The only apparent method of fabrication would be bonding of prefabricated stiffeners to a prefabricated skin. Alignment and perpendicularity of stiffeners would be difficult to maintain and this problem would be compounded if numerous stiffeners were bonded at one time in an effort to reduce labor costs and furnace time. Reinforcements on the ends of stiffeners and skins would be produced as described for zee construction. Fabrication of end attach fittings would involve extensive machining. Assembly of all three stiffened skin concepts would probably be accomplished on the tank "y" ring, with the edge splice joints made as the assembly progressed. This approach would ensure that the cone fit the tank.

2.6 Structural Concept Weights

Figures 28, 29, and 30 present weight breakdowns for the various methods of construction studied. Figure 31 is a summarization of total and elemental weights for all concepts and Figure 32 identifies the elements as percentages of cone weight. The data showed that titanium corrugated construction yielded the least cone weight with fiberglass honeycomb sandwich the second lightest, although approximately 100 pounds heavier. Fiberglass corrugated construction, using the forged fittings, was the third lightest. The stiffened skin concepts represented the heaviest structure.

Consideration of attachment details had a marked effect on total cone weight as evidenced by comparing Figure 17 with Figure 31. The initial weight

WEIGHT SUMMARY - CORRUGATED PANEL STRUCTURAL CONCEPTS
CRYOGENIC TANK SUPPORT

BASIC CORRUGATION MATERIAL	TITANIUM			FIBERGLASS		
NO. OF PANEL SPLICES	12			4		
TYPE OF PANEL SPLICES	Lap	Butt		Lap	Butt	
TYPE OF ATTACHMENT - PANELS TO SUPT. RING	Segmented Rings		Forged Fittings	Segmented Rings		Forged Fittings
ITEM/WEIGHT (LB)						
BASIC CORRUGATIONS	(306.0)	(306.0)	(306.0)	(235.0)	(235.0)	(235.0)
PANEL END STIFFENING	(18.6)	(18.6)	--	(93.0)	(93.0)	(93.0)
PANEL SPLICE	(3.7)+	(3.9)	(3.9)	(8.1)+	(1.3)	(1.3)
PANEL END FITTINGS, DOUBLERS & FAST.	(180.5)	(180.5)	(141.6)	(433.6)	(433.6)	(255.8)
Upper Ring Segments	53.3		--	170.5		--
Lower Ring Segments	51.9		--	166.8		--
Doublers	31.0		--	25.6		
Forged Fittings	--		72.7	--		158.0
Titanium Fasteners	20.6		53.7	37.8		49.2
Steel Lockbolts	23.7		15.2	32.9		48.6
ATTACHMENT - END FITTINGS TO SUPT. RING	(66.9)	(66.9)	(77.8)	(52.3)	(52.3)	(73.1)
Titanium Fasteners	15.9		59.7	17.6		54.3
Steel Lockbolts	13.9		18.1	15.0		18.8
Doubler Plates	37.1		--	19.7		--
"Y-RING" ΔWT.**				(54.8)	(54.8)	(54.8)
Total Basic Assembly	575.7	575.9	529.3	876.8	870.0	713.0
ΔWt. to all Steel Fasteners	13.5	13.5	42.0	20.2	20.2	38.2
Total Assy. Wt. with Steel Fasteners	589.2*	589.4	571.3	897.0*	890.2	751.2

* This weight assumes optional spot welding of panel end stiffeners. If these stiffeners are riveted to corrugations assy., the weight would increase from 10 to 19 pounds, dependent on rivet type.

** Titanium Corrugated Cone assumed to be baseline. Positive and Negative ΔWts. relate to this design.

\+ These weights include corrugation fillers (2.3 Lb. for Titanium & 7.2 Lb. for Fiberglass).

FIGURE 28

WEIGHT SUMMARY - HONEYCOMB PANEL CONCEPTS
CRYOGENIC TANK SUPPORT

BASIC SKIN MATERIAL	TITANIUM		FIBERGLASS	
TYPE OF CORE	HEX CELL FIBERGLASS			
CELL SIZE - IN.	3/16		3/8	
PANEL END FTG.	SEGMENTED TI. RING		LAMINATED FIB. FTG.	
NUMBER OF PANEL SPLICES	2			
ITEM/WEIGHT LB.				
BASIC HONEYCOMB PANEL	291.4		262.3	
Skin - Outer		52.8		67.5
Skin - Inner		52.4		66.6
Core		147.8		109.7
Adhesive (10 mil.)		38.4		18.5*
PANEL SPLICE	8.0		9.7	
Splice Plates		1.2		0.8
Edge Members		3.2		4.8
Fasteners		3.6		3.8
Inserts		--		.3
PANEL END STIFFENING & ATTACH.	386.1		306.7	
Laminated Ftgs.		--		221.2
Channel End Stiffeners		93.4		--
Segmented Attach. Rings		153.8		--
Attach. Ring Doublers		15.4		--
Support Attachment Plates		82.9		85.5
Attachment Plate Fillers		40.6		--
FASTENERS	101.2		67.7	
Panel - Steel Lockbolts		33.5		--
Supt. Ftg. - Titanium		67.7		67.7
"Y-RING" ΔWT.	-26.9		-14.1	
TOTAL BASELINE ASSEMBLY	759.8		632.3	
ΔWT. ASSUMING 15 MIL. ADHESIVE	+19.2		+9.2	
TOTAL (WITH 15. MIL. ADHESIVE)	779.0		641.5	

* Adhesive used only one one side.

FIGURE 29

WEIGHT SUMMARY - STIFFENED PANEL STRUCTURAL CONCEPT
CRYOGENIC TANK SUPPORT

STIFFENER TYPE	HAT		ZEE		BAR	
PANEL ATTACHMENT	← Milled Fittings →					
NO. OF PANEL SPLICES	8	4	8	4	8	4
BASIC PANEL MATERIAL	Ti.	Fib.	Ti.	Fib.	Ti.	Fib.
ITEM/WEIGHT - LB.						
BASIC PANEL	(551.6)	(397.2)	(608.0)	(474.0)	(544.6)	(500.7)
Skin	309.3	203.6	288.0	282.9	266.5	247.6
Stiffeners	237.5	189.6	315.0	183.9	278.1	253.1
Rivets*	4.8	4.0	5.0	7.2	--	--
PANEL END STIFFENING	--	(95.1)	--	(71.4)	--	(46.1)
Skin		24.6		22.1		25.0
Stiffeners		70.5		49.3		21.1
PANEL SPLICE PENALTY	(1.7)	(1.3)	(2.7)	(1.8)	(2.9)	(1.6)
PANEL END FITTINGS	(141.2)	(163.7)	(101.2)	(82.4)	(72.0)	(82.2)
Inner	61.2	66.5	51.5	34.6	38.6	31.6
Outer	80.0	97.2	41.9	36.6	33.4	50.6
Fillers	--	--	7.8	11.2	--	--
FASTENERS	(107.4)	(128.4)	(74.5)	(173.8)	(85.0)	(137.7)
Panel - Titanium	38.9	48.3	36.0	114.8	42.8	81.9
Panel - Steel	18.2	24.0	--	--	--	--
Supt. Ftg. - Titanium	25.0	27.7	18.6	30.7	20.6	28.6
Supt. Ftg. - Steel	25.3	28.4	19.9	28.3	21.6	27.2
"Y -RING" Δ WT.	(+3.1)	(+35.2)	(+24.8)	(+22.3)	(+26.9)	(+23.9)
TOTAL BASIC ASSEMBLY	805.0	820.9	811.2	825.7	731.4	795.2
Δ WT. TO ALL STL. FASTENERS	23.6	28.1	20.2	53.8	23.5	40.9
TOTAL (WITH STL. FASTENERS)	828.6	849.0	831.4	879.5	754.9	836.1

* These weights can be removed if optional bonded or spot weld stiffeners used.

FIGURE 30

CONICAL SUPPORT WEIGHT SUMMARY
CRYOGENIC TANK SUPPORT

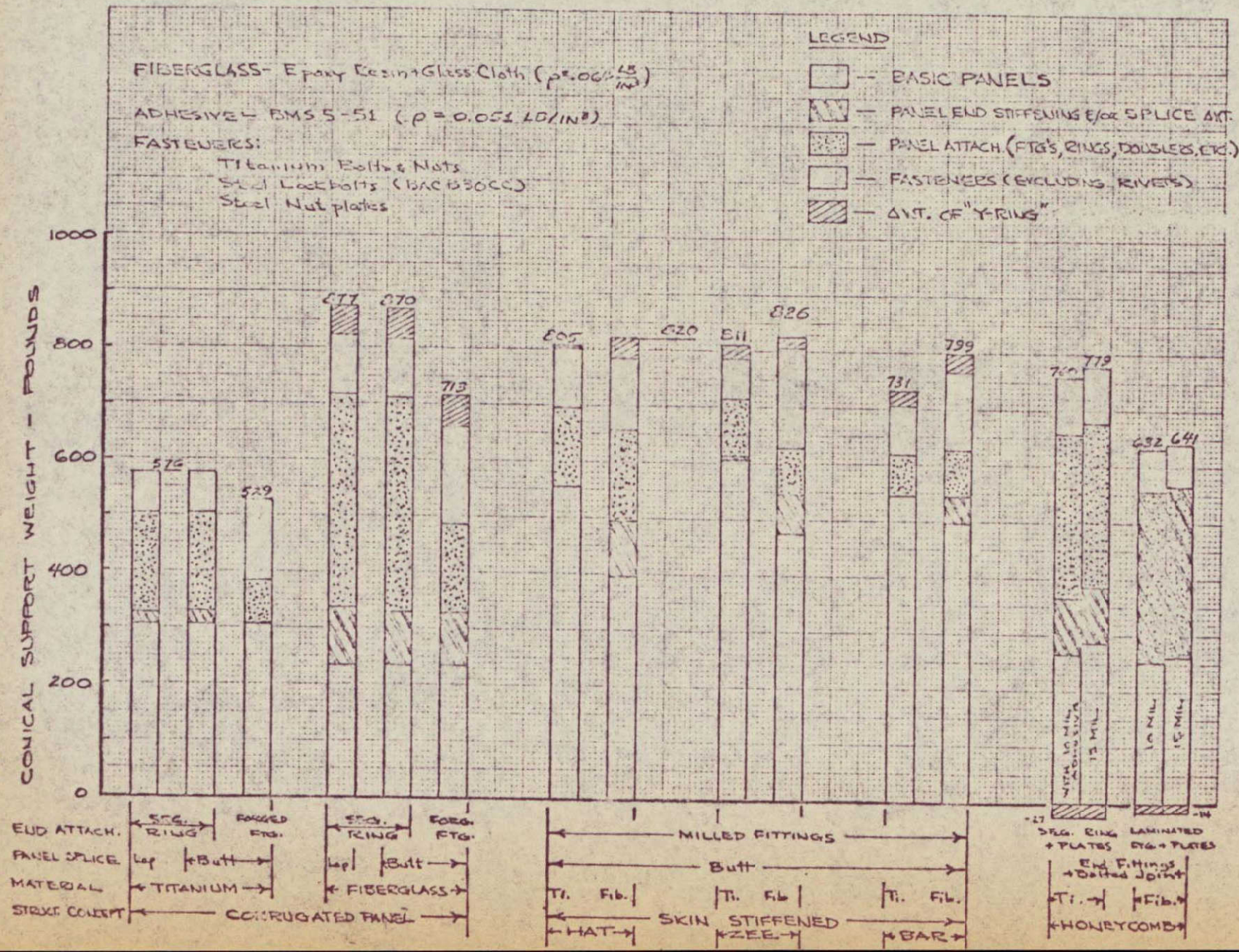

FIGURE 31

WEIGHT BREAKDOWN BY PERCENT
CONICAL SUPPORT SYSTEMS - CRYOGENIC
TANK SUPPORT

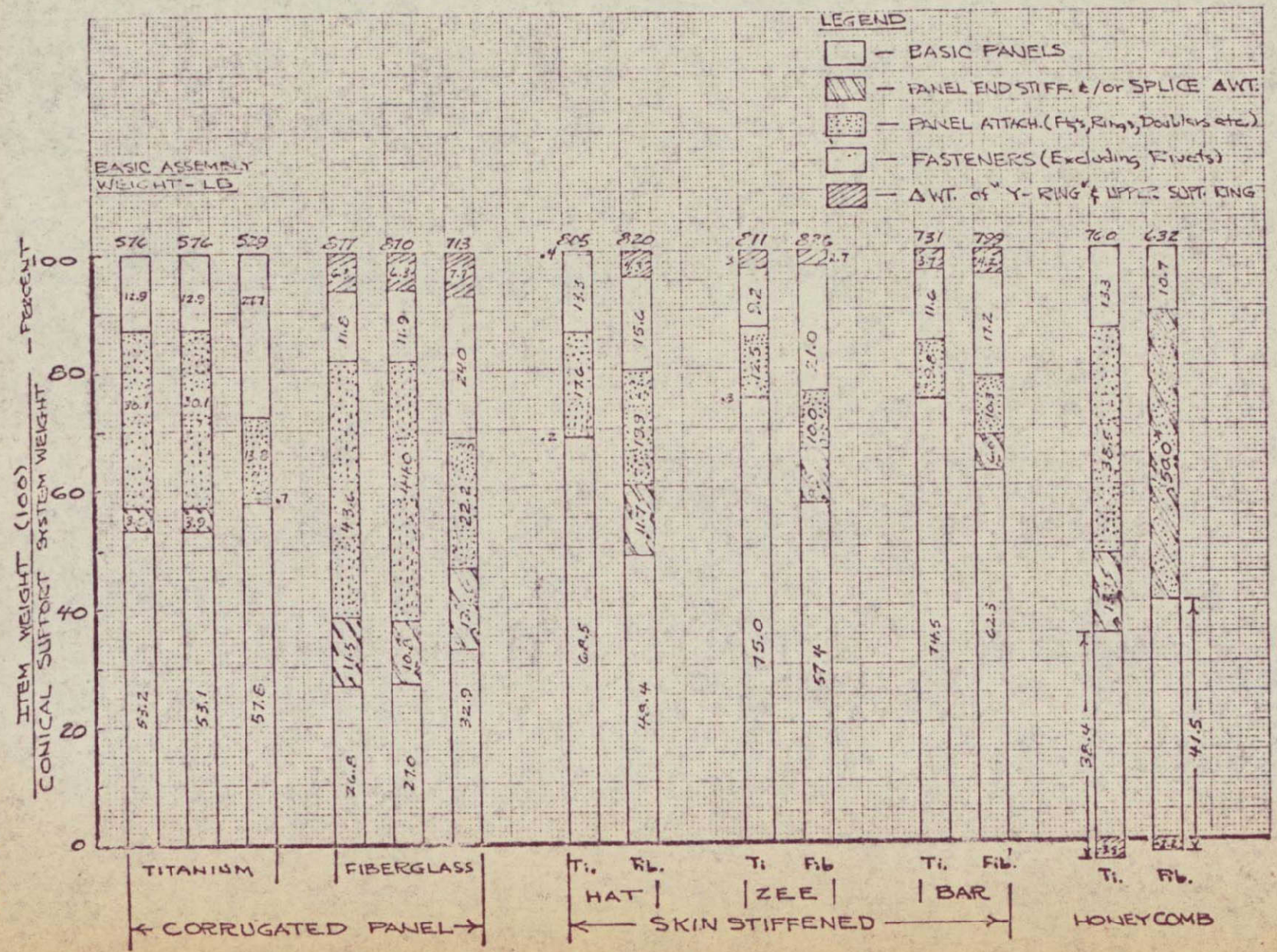

FIGURE 32

evaluation, which considered only the basic panel construction, indicated that corrugated titanium and fiberglass construction were the least weight, with titanium and fiberglass honeycomb sandwich a close second. When finalized designs were considered, the attachments and end stiffening increased the weight of the fiberglass corrugated and titanium honeycomb sandwich designs to less competitive positions. Edge attachments particularly penalized honeycomb sandwich construction.

Thermally induced strains were not accounted for in the titanium designs. It has been shown that thermal stresses were relatively high for titanium; thus the addition of an alleviating device (translating joint) could increase weight significantly. The corrugated titanium design could be the one exception in that it has the capability to expand and contract. Fiberglass thermal stresses were shown to be within the capacity of the material, therefore, translating designs were unnecessary and cone weights are realistic.

Weight comparisons alone could not be used to justify selection of a particular tank support structure since support heat leak greatly affected payload weight through boil-off losses. The scope of this contract did not allow a mission oriented parametric study to identify the relative importance of support weight and heat leak; however, it was possible to make comparisons based on certain assumptions.

It was assumed that support heat leak was essentially one-dimensional, (i.e., there was sufficient insulation of the proper design to thermally isolate the support), and therefore, the concepts could be compared in terms of hydrogen boil-off weight as well as structural weight. This simplified approach did not account for tank growth to compensate for boil-off losses or the alternate of operating the vessel at higher pressures; however, both of these approaches would increase inert weight and tend to degrade the higher heat leak supports

and enhance those with lower heat leak.

A second assumption was that the cone was sufficiently long to produce equilibrium temperatures of 37°R and 535°R at cold and warm ends respectively under steady state conditions.

The results of the heat flow analysis are presented in Figure 33. Conical support structural weights were added to hydrogen boil-off losses for weight totals. Fiberglass honeycomb sandwich provided the least total weight by a significant margin. The best titanium design was also honeycomb sandwich, however, the total weight was over 240% greater. Corrugated fiberglass construction was the second best approach but was 128% heavier than fiberglass honeycomb.

The total mission time was assumed to be 256 days, with the first 23 days allotted to nonvented pressure rise from top-off to operating pressure.

Heat flow was calculated using the length of cone between attachments to aluminum tank and support ring. This length varied depending upon end attachment design. No attempt was made to analyze heat flow across contact resistances such as bolted joints. The splice joint members contributed very little to total heat flow, thus the number of joints could be altered for manufacturing reasons with only slight thermal effect.

2.7 Subscale Conical Support Design

The final effort in Phase I was the preparation of a conical support detail design. In Phase II the support will be fabricated and delivered to MSFC. The support was designed to fit a 105 inch diameter tank and tapered to approximately 117 inches at the large end. This part was intended primarily for thermal performance tests. The cross section shape, thickness and material gages were

	Configuration	Weight (Lb)	Heat Flow (Btu/Hr.)*	H_2 Boiloff Wt.** (Lb)	Σ Weight (Lb)	Heat Flow Ratio Opposite Mat'l Counter Part	Splice Joint % of Total Cone Heat Flow
Fiberglass	Honeycomb	632	16.5	476	1108		0.43
	Corrugated-Butt Joints + "Y" Ring Attach.	870	26.7	771	1641		.46
	Corrugated-Lap Joint "Y" Attach. Rings	877	26.7	771	1648		0.24
	Corrugated-Butt Joints + Forged Rs	713	24.6	710	1423		0.46
	Hat Stiffened	821	32.6	940	1761		0.27
	Zee Stiffened	826	40.7	1175	2001		0.29
	Bar Stiffened	795	43.7	1260	2055		0.24
Titanium	Honeycomb	760	66.9	1930	2690	4.1/1	1.28
	Corrugated-Butt Joints + "Y" Ring Attach	576	161.5	4660	5236	6.1/1	1.22
	Corrugated-Lap Joints "Y" Ring Attach	576	160.2	4630	5206	6.0/1	0.41
	Corrugated-Butt Joints Forged Rs	529	161.5	4660	5189	6.6/1	1.22
	Hat Stiffened	805	286.3	8270	9075	8.8/1	0.45
	Zee Stiffened	811	343.3	9910	10721	8.4/1	0.38
	Bar Stiffened	731	296.4	8560	9291	6.8/1	0.45

* Mean Thermal Conductivity Titanium = 0.24 $\frac{\text{Btu-In}}{\text{In}^2\ \text{Hr.}\ {}^{\circ}\text{R}}$

** 5600 Hour Mission

FIGURE 33

the same as the 32 ft counterpart as was the cone length. This was done in an effort to produce the same heat leak per inch of cone circumference in the subscale test article as in the full scale part. Fiberglass honeycomb sandwich with fiberglass face skins was shown to be the most promising concept in the study; therefore, the subscale cone utilized these materials. Figure 34 is a drawing of the part.

A four segment design was adopted rather than the two segments used in the full size cone of Figure 23. This was done to simplify tool fabrication and handling as well as to reduce the amount of materials committed to a single cure cycle. The increase in full size cone heat flow due to the extra joints was shown (in Figure 33) to be minor. Changes to reduce fabrication costs included (1) the substitution of NAS 501 stainless steel bolts for titanium and A286 bolts, (2) elimination of nut plates along one side of each segment joint, and (3) the substitution of Volan A finish for 901 finish on the "S" glass cloth used to fabricate laminate face skins and edge members. The Volan finish results in a laminate with somewhat lower strength, however, the properties were more than adequate for the design.

A 10 mil layer of modified epoxy adhesive film (AF 131) was added to the subscale cone design to promote adhesion of the preimpregnated face skin laminate to honeycomb core. This technique was recommended by the prepreg supplier because the E-787 resin system did not have particularly good filleting characteristics.

3.0 CONCLUSIONS AND RECOMMENDATIONS

The study results showed that fiberglass construction was the more weight-efficient design in all cases when both structural and boiloff weights were considered. This was due largely to the low thermal conductivity of the material. Fiberglass honeycomb sandwich construction was the best design approach considered.

An analysis to determine potential structural weight savings based on configuration cross section alone will not yield realistic results. The effect of edge members, reinforcements and fasteners can increase basic structural weight by more than 100% as evidenced for honeycomb sandwich and corrugated fiberglass support designs.

Stiffened skin designs were considered the most easily fabricated and the corrugated designs probably the most difficult. Honeycomb sandwich fabrication was essentially state of the art; however, the integral, tapered edge attachment laminate added complexity.

Clearance between conical support and tank head was very limited. This was expected to cause problems in insulating the support and could reduce its thermal isolating effectiveness. Several alternatives were possible. These were: (1) lengthening the aluminum "y" ring with an attendant weight penalty, (2) relocation of the "y" ring to a more forward position on the tank head, or (3) lengthening the conical support to account for some loss of isolation capability at the cold end. It is recommended that a thorough stress and thermal analysis of this joint be conducted after insulation designs are developed. This will provide insight into the magnitude of the problem and identify advantages or disadvantages in some of the alternatives suggested.

Fiberglass honeycomb sandwich construction is recommended for fabrication of the 105-inch conical support in Phase II of this program.

4.0 REFERENCES

1. Goodyear Aerospace Corp., "Program for the Evaluation of Structural Reinforced Plastic Materials at Cryogenic Temperatures", Contract NAS 8-11070 for NASA/MSFC, GER 12792, August 1966.

2. Bartlett, Donald H., "Nonmetallic Parts for Launch Vehicles and Spacecraft Structures", Contract NAS 8-18037 for NASA/MSFC, Boeing Document No. D2-114155-1.

3. Seide, P., Weingarten, V. I., and Morgan, E. J., "Final Report on the Development of Design Criteria for Elastic Stability of Thin Shell Structures", Space Technology Laboratories, Inc., Report STL/TR-60-0000-19425, December 1960.

4. Block, D. L., "Buckling of Eccentrically Stiffened Orthotropic Cylinders Under Pure Bending", NASA TND-3351, March 1966.

5. Douglas Aircraft Co., "Design Concepts for Minimum Weight High Performance Supersonic Aircraft Structures", Vol. I ASD-TDR-63-871, September 1963, ASTIC 036226.

6. Gerard, George, and Becker, Herbert, "Handbook of Structural Stability Part I - Buckling of Flat Plates", NACA TN 3781, July 1957.

7. Roark, R. J., "Formulas for Stress and Strain", 4th Edition, McGraw-Hill Book Company

8. Peterson, James P., and Card, Michael F., "Investigation of the Buckling Strength of Corrugated Webs in Shear", NASA-TND-424, June 1960.

9. Apollo Program Office, "Structural Systems and Program Decisions", NASA SP-6008 pp. L1-L8, June 1966, ASTIC 036634.

10. Shanley, F. R., "Weight Strength Analysis of Aircraft Structures", Dover Publications Inc., Second Edition, 1960.

11. Koelle, "Handbook of Astronautics", Section 22, Structural Analysis by Hellebrand, E. A., McGraw-Hill Book Co., 1961.

12. Farrar, D. J., "The Design of Compression Structures for Minimum Weight", Journal of the Royal Aeronautical Society, November 1949.

13. Bleich, Friedrich, "Buckling Strength of Metal Structures".

14. Timoshenko and Gere, "Theory of Elastic Stability".

15. Anon., "Composite Construction for Aircraft, Part III - Design Procedures" MIL-HDBK 23, U.S. Dept. of Defense, Nov. 1961 (Revised Oct. 1962).

16. Peterson, J. P., and Anderson, J. K., "Structural Behavior and Buckling Strength of Honeycomb Sandwich Cylinders Subjected to Bending".

17. Bruhn, E. F., "Analysis and Design of Flight Vehicle Structures", Tri-State Offset Co., 1965.

18. Anon., "Sandwich Construction for Aircraft" Part II Materials Properties and Design Criteria MIL-HDBK-23, U. S. Dept. of Defense, 2nd Edition, 1955.

19. Weingarten, V. I., Morgan, E. J., and Seide, P., "Elastic Stability of Thin Walled Cylindrical and Conical Shells Under Axial Compression", AIAA Journal, Vol. 3, No. 3, March 1965.